Article:
Medici, G, West, LJ and Mountney, NP orcid.org/0000-0002-8356-9889 (2016) Characterizing flow pathways in a sandstone aquifer: Tectonic vs sedimentary heterogeneities. Journal of Contaminant Hydrology, 194. pp. 36-58. ISSN 0169-7722

https://doi.org/10.1016/j.jconhyd.2016.09.008

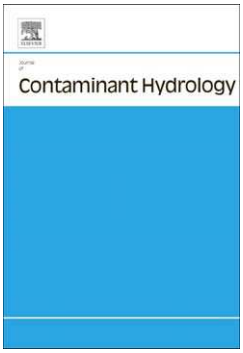

Characterizing flow pathways in a sandstone aquifer: Tectonic vs sedimentary heterogeneities

G. Medici, L.J. West, N.P. Mountney

PII: S0169-7722(16)30213-3
DOI: doi: 10.1016/j.jconhyd.2016.09.008
Reference: CONHYD 3250

To appear in: *Journal of Contaminant Hydrology*

Received date: 1 May 2016
Revised date: 9 September 2016
Accepted date: 20 September 2016

Please cite this article as: Medici, G., West, L.J., Mountney, N.P., Characterizing flow pathways in a sandstone aquifer: Tectonic vs sedimentary heterogeneities, *Journal of Contaminant Hydrology* (2016), doi: 10.1016/j.jconhyd.2016.09.008

Characterizing flow pathways in a sandstone aquifer: tectonic vs sedimentary heterogeneities

G. Medici[a]*, L.J. West[a], N.P. Mountney[a]

[a] School of Earth and Environment, University of Leeds, Woodhouse Lane, Leeds, W Yorkshire, LS2 9JT, UK

*Corresponding author at: School of Earth and Environment, University of Leeds, Leeds LS 9TJ, United Kingdom.
E-mail address: eegm@leeds.ac.uk (Giacomo Medici)

Abstract

Sandstone aquifers are commonly assumed to represent porous media characterized by a permeable matrix. However, such aquifers may be heavy fractured when rock properties and timing of deformation favour brittle failure and crack opening. In many aquifer types, fractures associated with faults, bedding planes and stratabound joints represent preferential pathways for fluids and contaminants. In this paper, well test and outcrop-scale studies reveal how strongly lithified siliciclastic rocks may be entirely dominated by fracture flow at shallow depths (≤ 180 m), similar to limestone and crystalline aquifers. However, sedimentary heterogeneities can primarily control fluid flow where fracture apertures are reduced by overburden pressures or mineral infills at greater depths.

The Triassic St Bees Sandstone Formation (UK) of the East Irish Sea Basin represents an optimum example for study of the influence of both sedimentary and tectonic aquifer heterogeneities in a strongly lithified sandstone aquifer-type. This fluvial sedimentary succession accumulated in rapidly subsiding basins, which typically favours preservation of complete depositional cycles including fine grained layers (mudstone and silty sandstone) interbedded in sandstone fluvial channels. Additionally, vertical joints in the St Bees Sandstone Formation form a pervasive stratabound system whereby joints terminate at bedding discontinuities. Additionally, normal faults are present through the succession showing particular development of open-fractures. Here, the shallow aquifer (depth ≤180 m) was characterized using hydro-geophysics. Fluid temperature, conductivity and flow-velocity logs record

inflows and outflows from normal faults, as well as from pervasive bed-parallel fractures. Quantitative flow logging analyses in boreholes that cut fault planes indicates that zones of fault-related open fractures characterize ~ 50% of water flow. The remaining flow component is dominated by bed-parallel fractures. However, such sub-horizontal fissures become the principal flow conduits in wells that penetrate the exterior parts of fault damage zones, as well as in non-faulted areas.

The findings of this study have been compared with those of an earlier investigation of the deeper St Bees Sandstone aquifer (180 to 400 m subsurface depth) undertaken as part of an investigation for a proposed nuclear waste repository. The deeper aquifer is characterized by significantly lower transmissivities. High overburden pressure and the presence of mineral infillings, have reduced the relative impact of tectonic heterogeneities on transmissivity here, thereby allowing matrix flow in the deeper part of the aquifer. The St Bees Sandstone aquifer contrasts the hydraulic behaviour of low-mechanically resistant sandstone rock-types. In fact, the UK Triassic Sandstone of the Cheshire Basin is low-mechanically resistant and flow is supported both by matrix and fracture. Additionally, faults in such weak-rocks are dominated by granulation seams representing flow-barriers which strongly compartmentalise the UK Triassic Sandstone in the Cheshire Basin.

Key words: Sandstone, flow pathways, heterogeneities, fault, fracture, matrix

1. Introduction

Quantitative studies for gaining an improved understanding of flow pathways represent a key issue for groundwater protection and catchment planning for all aquifer types. This work focuses on lithified sandstone aquifers and aims to characterize the role various types of sedimentary and tectonic heterogeneities on aquifer behaviour and contaminant transport in the phreatic zone. The rate of passage of inorganic (e.g., NAPL, nitrogen, phosphate and chlorinated solvents) and organic (e.g., bacteria, virus) contaminants flowing through a sandstone matrix are controlled by a range of sedimentary heterogeneities (Lawrence et al., 2006; Mobile et al., 2016; Qin et al., 2013; Rivett et al., 2011; Tellam and Barker, 2006; Zhu and Burden, 2001), such as the presence of relatively low permeability mudstone layers. Alternatively, these contaminants may be transported at higher flow velocities along mechanical discontinuities of tectonic origin, such as bedding parallel fractures, vertical joints or fault-related fracture corridors (Barker et al., 1998; Berkowitz, 2002;

Bradbury et al., 2013; Cilona et al., 2015; Faulkner et al., 2009; Hartmann et al., 2007; Huyakorn et al., 1994; Odling and Roden, 1997; Rutqvist and Tsang, 2003; Steele and Lerner, 2001). The relative importance of matrix versus fracture flow is known to vary as a function of depth, owing to different sensitivities to geochemical alteration (e.g., diagenesis) and overburden pressure (Akin, 2001; Howard, 1988; Zoback and Byerlee, 1975). Thus, a specific study, which combines hydraulic tests (pumping tests, flow logging) at different depths, may provide an improved understanding of the relative importance of porous matrix versus fractures in controlling groundwater flow and contaminant transport in sandstone aquifers (Gellash et al., 2013; Tellam and Barker, 2006). Multi level sampling arrays have been used to detect traces of contaminants in relation to bedding parallel fractures in sandstone aquifers (e.g., Gellash et al., 2013; Powell et al., 2013). The hydrogeology of faults represents a further specific key issue in groundwater protection since such structural discontinuities can act as either barriers or preferential pathways for contaminants (Bense et al., 2013; Bottrell et al., 2008; Caine et al., 1996; Mohamed and Worden, 2006). Furthermore, water wells have been recognized both as preferential pathways for and sources of contaminants (Avci, 1992). Hence, pollutant plumes may be exacerbated by the interaction between groundwater and boreholes (Avci, 1992; Hammond, 2016; Rivett et al., 1990). The use of well tests in a fractured media allows us to test the interaction between all preferential pathways for contaminant transport which are represented by boreholes, tectonic open fractures and permeable sedimentary layers (Bauer et al., 2004; Odling et al., 2013).

Previous quantitative studies, involving hydraulic tests in lithified sandstone aquifers (Brassington and Walthall, 1985; Gellash et al., 2013; Hitchmough et al., 2007; Lo et al., 2014; Price et al., 1982; Runkel et al., 2006), have focused on determining only the role of sub-horizontal discontinuities on water flow, including their connections through vertical stratabound joints. In contrast, past studies of the hydrogeology of faults in sandstone aquifers have focused on plug-scale fault rock samples and mini-permeameter outcrop experiments. Such studies have aimed to quantify the sealing potential of normal faults on hydrocarbon reservoir analogues (e.g., Antonellini et al., 1994; Balsamo and Storti, 2010; Torabi and Fossen, 2009; Tueckmantel et al., 2012). Consequently, quantitative hydraulic studies that encompass multiple aquifer heterogeneities, such as sub-horizontal stratigraphic discontinuities linked by multi-layer vertical fractures and extensional faults, are lacking.

This work investigates the sandstone aquifer of the Triassic St Bees Sandstone Formation, which represents the basal part of the Sherwood Sandstone Group – the second most important UK aquifer in terms of the amount of groundwater abstracted (Allen et al., 1997; Binley et al., 2002; Smedley et al., 2002). The Sherwood Sandstone Group has been the object of recent studies of sedimentary heterogeneities (e.g., Medici et al., 2015; Newell et al., 2016; Wakefield et al., 2015). Results from these works have demonstrated how the St Bees Sandstone Formation represents an optimum analogue for the characterization of sedimentary heterogeneity in analogous subsurface hydrocarbon reservoirs of fluvial origin that accumulated in rapidly subsiding basins, such as those of the East Irish Sea Basin (Akhurst et al., 1998; Chadwick et al., 1994). Such conditions typically allow preservation of low-permeability units, including mudstone lenses that occur interbedded in otherwise sandstone-dominated successions (Colombera et al., 2013; Miall, 1977). Notably, the St Bees Sandstone aquifer is entirely characterized by a stratabound fracturing system (*sensu* Gillespie et al., 2001; Odling et al., 1999; Odonne et al., 2007; Rustichelli et al. 2013, 2016), which is particularly pervasive in this aquifer due to its layered nature coupled with high mechanical resistance (Ameen, 1995; Bell, 1992; Daw et al., 1974). Fault zones in this aquifer are characterized specifically by the development of open fractures and a paucity of low-porosity deformation bands (Knott, 1994). Consequently, the St Bees Sandstone aquifer represents an optimum laboratory to test a wide range of aquifer heterogeneities of both tectonic (e.g., vertical joints, bedding parallel and extensional fractures) and sedimentary origin (e.g., mudstone layers), which are especially well represented in this aquifer (Ameen, 1995; Bell, 1992; Jones and Ambrose, 1994; Knott, 1994; Medici et al., 2015). Additionally, parts of the St Bees Sandstone aquifer that are buried at depths greater than 180 m, have been the object of a hydro-geophysical characterization, which commenced in the early 1990s as part of the planning of the proposed Sellafield nuclear waste repository (e.g., Appleton, 1993; Michie, 1996; Milodowski et al., 1998; Nirex, 1992 a, 1992b, 1992c, 1993a, 1993b, 1993c; Streetly et al., 2000, 2006). Thus, this study area offers the opportunity to compare hydro-geophysical studies undertaken at different depths, thereby allowing the opportunity to distinguish the depth-sensitivity of tectonic flow pathways versus matrix flow.

Specific research objectives are as follows: (i) use hydro-geophysics to constrain all the potential flow heterogeneities using imaging and wireline well-logs; (ii) quantify the role of individual structure types in terms of their contribution to flow using fluid temperature, conductivity and velocity logs; (iii) compare the hydro-geophysical characterization undertaken at shallow depths (≤150 m) as an outcome of this work, with previous studies that characterized the aquifer properties at greater depths (180 to 400 m); and (iv) compare the hydraulic characteristics of the St Bees Sandstone aquifer with those of less-mechanically resistant sandstone aquifers.

2. Hydrogeological background

The Sherwood Sandstone Group (Lower Triassic) is a red-bed succession that has long been ascribed to a mixed fluvial and aeolian origin (e.g., Bashar and Tellam, 2011; Ixer et al., 1979; Mountney and Thompson; 2002; Tellam and Barker, 2006; Thompson, 1970; Turner, 1981). This sandstone-dominated succession represents the UK's second most important aquifer. Contamination has arisen due to agricultural activity, and the release of industrial waste and sewage in urban areas (Barrett et al., 1999; Bottrell et al., 2008; Bloomfield et al., 2001; Cassidy et al., 2014; Gooddy et al., 2002; Powell et al., 2003; Rivett et al., 1990; Rivett et al., 2012; Zhang and Hiscock, 2010, 2011). In West Cumbria (Fig. 1a, b), the Sherwood Sandstone Group attains a typical thickness of 1300 m (Jones and Ambrose, 1994; Nirex, 1997) and is formally divided into three different formations: the St Bees, Calder and Ormskirk Sandstone formations (Barnes et al., 1994; Holliday et al., 2008). The St Bees Sandstone aquifer, which is the focus of this study, is predominantly characterized by fine- to medium-grained sandstone of fluvial origin that passes upwards into the aeolian-dominated succession of the overlying Calder Sandstone Formation (Jones and Ambrose, 1994; Holliday et al., 2008). The Cumbrian Coastal Group, which underlies the St Bees Sandstone aquifer, is characterized by shale and gypsum, anhydrite and dolomite evaporite deposits, and represents a basal aquiclude lithology for the St Bees Sandstone aquifer (Fig. 1; Holliday et al., 2008; Smith, 1924; Strong et al., 1994).

The field site is located in the St Bees-Egremont area in NW England (Fig. 1a, b) where the St Bees Sandstone aquifer is confined by glacial and alluvial Quaternary deposits (McMillan et al., 2000). The St Bees Sandstone Formation is divided into two members: the North Head Member and the overlying South Head Member

(*sensu* Medici et al., 2015). The two members are differentiated primarily based on the abundance of fine-grained mudstone layers which range in grain size from clay to coarse silt (Ambrose et al., 1994; Medici et al., 2015; Nirex, 1997). The basal 35 m of the lower North Head Member is arranged into an alternation of fine-grained sandstone and mudstone beds. This basal part of the aquifer passes upwards into a succession dominated by sandstone, with mudstone layers representing only 10% and 5% of the entire succession in the upper North Head and South Head members, respectively (Barnes et al., 1994; Jones and Ambrose, 1994; Nirex, 1997). Water boreholes in the St Bees Sandstone aquifer of West Cumbria are designed with long screens (80-150 m) to penetrate only the South and upper part of the North Head members aiming to avoid the potential low permeability unit which is represented by the mud-prone lower part of the North Head Member (Allen et al., 1997).

Tectonic heterogeneities, which characterize the UK Sherwood Sandstone aquifer, are represented by normal faults and stratabound joints (Allen et al., 1998; Chadwick, 1997). On a local scale, detailed studies of the tectonic structures of the St Bees Sandstone Formation have been undertaken by Knott (1994), Ameen (1995) and Gutmanis et al. (1998) as part of a series of radioactive waste disposal assessments associated with the Sellafield repository. These studies confirm the typical pattern of tectonic structures of the UK Sherwood Sandstone, for which high-angle normal faults and stratabound joints characterize the studied aquifer.

Knott (1994) highlights the relatively minor occurrence of granulation seams (*sensu* Beach et al., 1999; Hitchmough et al., 2007; Knott et al., 1996; Pittman, 1981) in the fault zones of the St Bees Sandstone Formation compared to deposits of the Sherwood Sandstone Group across the UK more widely, where such tectonic structures are more abundant (Griffiths et al., 2016; Knott, 1994). Stratabound joints, which characterize the entire aquifer, have been related in the study area to the Cenozoic uplift of NW Europe (Barnes et al., 1994; Nirex, 1997). Additionally, the fracture network which characterizes the St Bees Sandstone aquifer also includes bedding and cross-bedding fractures. These sub-horizontal discontinuities are related to the opening of sedimentary discontinuities due to reduction of the vertical stress tensor in response to the Cenozoic lithospheric uplift of NW Europe (Allen et al., 1998; Ameen, 1995; Duperret et al., 2012; Gillespie et al., 2001; Odling et al., 1999). Layered aquifers of the north-western European region are typically characterized by similar fracturing patterns (e.g., Duperret et al., 2012; Gillespie et

al., 2001; Odling et al., 1999). The Sherwood Sandstone Group across the UK presents typical matrix hydraulic conductivity and porosity values of 0.1-8.0 m/day and 15 to 30%, respectively (e.g., Allen et al., 1997; Bloomfield et al., 2006; Pokar et al., 2006). Shear strength is typically characterized by low values ranging from over-consolidated sand to weak rock (Hawkins et al., 1992; Yates, 1992). In this hydro-mechanical framework, the St Bees Sandstone aquifer of West Cumbria represents an exception in the red-bed successions of the UK Sherwood Sandstone Group. Indeed, the interquartile range for plug-scale hydraulic conductivity ranges from 3.0×10^{-4} to 2.5×10^{-2} m/day and from 13% to 20% for porosity, these value are much lower compared to the petrophysical properties of the Sherwood Sandstone Group across other parts of the UK (Allen et al., 1997). Furthermore, the St Bees Sandstone Formation is relatively mechanically resistant; it is commonly used as a building stone in the West Cumbrian region (Bell, 1992). Additionally, Daw et al. (1974) has demonstrated, using multi-stage triaxial stress experiments, how the West Cumbrian St Bees Sandstone aquifer is characterized by the typical petro-mechanic characteristic of lithified clastic rock at moderate depths (cf., Crook and Howell, 1977; Jones, 1975). As a consequence, intergranular permeability is only slightly reduced (by 6%) in response to an increase in lithostatic pressure of 7 MPa, representing the overburden pressure at approximately 300 m below the surface (Daw et al., 1974). By contrast, the fracture flow component is substantially removed (by 90%) in experiments that apply the same amount of overburden pressure (7MPa) to plugs of the St Bees Sandstone Formation that contained single fractures (Daw et al., 1974).

Large-scale hydraulic tests in the Sherwood Sandstone Group of West Cumbria are summarized by Allen et al. (1997) with regards to shallow water wells. However, Streetly et al. (2000) investigated the more deeply buried parts of the St Bees Sandstone aquifer in the context of an investigation for a proposed radioactive waste repository at Sellafield. The two different groups of pumping tests data described by Allen et al. (1997) and Streetly et al. (2000) show different transmissivities. These hydraulic tests were undertaken at shallow (zero to 200 m) and greater (200 to 400 m) depths and show a decreasing transmissivity with increasing subsurface depth of two orders of magnitude (10^2). Furthermore, pumping tests undertaken by Streetly et al. (2000) on the deep St Bees Sandstone aquifer as part of the planning for the Sellafield radioactive waste repository show how the stratigraphic units of the North

Head Member which are characterized by a higher occurrence of mudstone beds are also characterized by relatively lower aquifer transmissivity (T= 0.46 - 1.99 m^2/day; median = 1.30; σ = 1.42; n=23). In contrast, the South Head Member of the St Bees Sandstone Formation (which is dominated by channel-sandstone deposits) is characterized by aquifer transmissivities ranging from 1.17 up to 4.88 m^2/day (median = 1.73; σ = 1.31; n=9). The fact that no systematic comparison of these datasets has been undertaken previously, so as explain the depth dependence of transmissivity is part of the rationale for the work reported in this paper. Additionally, the interpretation of variations in transmissivity as function of depth is coupled in this work with the quantification of the different contribution of tectonic structures (faults, bedding fractures and joints) on water flow at shallow depths (≤ 180 m).

3. Experimental methods

3.1 Wireline and optical televiewer logging

Six pre-existing monitoring wells (0.15 to 0.20 m in diameter; 90 to 152 m depth), which are located at different distances from mapped fault traces, were geophysically logged (Fig. 1b; Tab. 1). Mechanical calliper, natural gamma, resistivity, gamma-gamma density, neutron porosity and optical televiewer (ALT QL40 mk5) logs were recorded, along with the structure picking (*sensu* Williams and Johnson, 2004) of both sedimentary and tectonic heterogeneities, to characterize the orientation of geological heterogeneities. This structure picking allowed plotting of open fractures (n = 583), thin white sandstone beds (n = 279) and thin red mudstone beds (n = 28), as well as the calculation of vector mean statistics for the orientation of each group of heterogeneities using the Stereonet 9 software package (Allimendinger et al., 2012). Fractures present in the St Bees Sandstone, and recorded in the logs, comprised bedding plane fractures, cross bedding fractures, vertical joints and fault related-open fractures. Granulation seams were not detected by the automated structure picking procedure since such tectonic structures occur in only one well (Ellergill Bridge) as tortuous and short (0.05-0.1 m) bands that do not fully cut across the entire borehole width.

3.2 Scanlines-stratabound joints at cliff outcrops

Scan-line surveys have been performed at cliff outcrops around St Bees Head (see Fig. 1) to characterize the stratabound fracturing system present in the St Bees

Sandstone aquifer, since vertical boreholes numerically underestimate sub-vertical fractures (Terzaghi, 1965). The chosen methodology is specific for stratabound joints (Rustichelli et al., 2013) and involves the recording of 5 parameters: strike orientation, dip inclination, fracture horizontal spacing distance, percentage of infilled fractures and the thickness of the mechanical layer which contains the joints. Ten scanlines were measured along five different study sites (at each site two orthogonal horizontal scanlines lines have been realised to avoid bias). A total of 188 discontinuities which includes sub-vertical joints (n=140), cross (n=21) and bedding parallel (n=27) fractures were recorded and plotted on stereonets (cf., Allimendinger et al., 2012).

3.3 Pumping tests

Historical single-borehole pumping test data from the studied wells have been re-analysed using the ESI AquiferWin32 V.5 software package to obtain reliable transmissivity values to use for a quantitative flow-log analysis. Step tests have been analysed using the method of Eden and Hazel (1973) and the associated recovery using the method of Theis (1935). Data from pumping tests characterized by a constant abstraction flow are also available; for these data the recovery phase has been analysed using the Theis methodology.

Furthermore, the analysed pumping tests have been integrated with previously published pumping test data also acquired, to characterize the St Bees Sandstone aquifer more fully (Allen et al., 1997; Streetly et al., 2000). This was done to characterize transmissivity ranges from the shallow (n = 21) and the deep (n = 32) parts of the aquifer.

3.4 Upscaling hydraulic conductivity

Transmissivity values from well tests are compared with upscaled values derived from hydraulic conductivities that are available in literature for the St Bees Sandstone aquifer in West Cumbria, to establish the relative contribution of fracture versus matrix flow in the shallow aquifer (Allen, 1997; Nirex, 1992a, 1992c, 1993b, 1993c). The horizontal hydraulic conductivity from sandstone plugs was upscaled using the geometric mean for the screen length (Tab. 1) of each flow-logged well to compute the screen transmissivity. Flow in this upscaling approach is assumed perpendicular to the screen consistent with the layered nature of the aquifer and sub-

horizontal dip of the beds (10°). Geometric and harmonic means are typically used for upscaling of hydraulic permeability in heterogeneous sandstone aquifer or reservoir types (Chen et al., 2003; Jackson et al., 2003). We used the geometric mean since better represents the sensitivity of horizontal flow to layer permeability variation. For example, Zheng et al. (2000) has found a better match between plug and field scale transmissivity upscaling the K_h geometric mean rather than K_h harmonic mean in sandstone fluvial reservoirs.

3.5. Temperature, conductivity and flow velocity logs

Both pumped and ambient-flow velocity, fluid temperature and conductivity logs have been recorded in all six study wells using a Geovista mk2 impeller flow meter (minimum observable flow rate of 10 mm/s according to the manufacturer). Flow-log analyses aimed to determine the hydraulic conductivity (k_i) of each identified hydraulic layer i, with thickness (Δz_i) from the computed partial transmissivity (T_i) using equation (1),

$$T_i = k_i \times \Delta z_i \quad (1)$$

A quantitative approach has been used to analyse flow meter data to determine partial transmissivity (T_i) by combining overall well transmissivity values derived from the pumping test analyses with fluid velocity logs. The quantitative method adopted for the flow log analysis comprises a model to determine transmissivity value of fracture rock zones (Paillet, 1998, 2000). Day-Lewis et al. (2011) provides a computer program for the latter model, called “Flow-Log Analysis of Single Holes (FLASH)”. This program is based on the multi-layer Thiem (1906) equation (2), which describes confined radial flow in both ambient and stressed flow conditions,

$$Q_i = \frac{2\pi T_i(h_w - h_i)}{\ln(r_0/r_w)} \quad (2)$$

where Q_i is the volumetric flow into or out of the well from layer i; h_w and h_i are, respectively, the hydraulic head in the well (which has radius r_w) and in the far-field at r_0 (the radius of influence); T_i is the transmissivity of layer i. The FLASH program has an optimizing calibration method which aims to minimize difference between

data and model misfit. The model misfit is generated based on the differences (h_w-h_i) between the water level in the borehole (h_w) under pumped and ambient conditions and the far-field heads (h_i). The automated model calibration of the FLASH program is based on a Generalized Reduced Gradient algorithm which was developed by Lasdon and Smith (1992). Four of the six wells examined did not show significant diameter variations, but in two cases (Black Ling, Pallaflat Reservoir wells) diameter variations > 30% occurred in correspondence of faults in thick intervals (2-5 m). Here, water flow (Q_i) was manually corrected for these borehole diameter changes.

Drawdowns in the wells between pumped and ambient conditions are assumed to represent aquifer drawdowns; head losses between the well and the aquifer (skin effects, wells losses) are assumed to be small. Additionally, the FLASH program requires information concerning well construction (top and bottom elevations of open section, well diameter), depth of the water table and an estimate of the radius of influence of pumping (r_o=50 - 165 m)[1] in each borehole.

The Day-Lewis et al. (2011) methodology has been applied to flow-log analyses in four of the six wells (Black Ling, Bridge End Trial, Rottington Trial, Thornhill Trial), which all showed strong flows under ambient conditions (up to 80 mm/s upflow). This is consistent with the results of Brassington (1992) who found significant ambient upflows in open wells in the study area. However, logs carried out in the two remaining wells (Ellergill Bridge, Pallaflat Reservoir) could not be successfully analysed using the Day-Lewis et al. (2011) methodology, possibly due to lower ambient flow rates (0-18 mm/s)[2]. Hydraulic effects associated with irregular borehole diameter and resulting changes in flow velocity which may trigger water turbulence may also have contributed (Grass, 1971, Paillet, 2004, Tsang et al., 1990). Instead, these well logs were analysed using a simpler approach that assumes quasi-steady state flow in pumped conditions, but negligible head difference between layers and vertical ambient flow in the borehole, and hence only requires data from the pumped flow-logs (Molz et al., 1989; Fienen et al., 2004; Parker et al., 2010). This methodology determines the transmissivity T_i for each layer, simply from the proportion of total inflow to the well entering from that layer under pumped

[1] Radius of influence for the entire pumped interval was found using the transient flow equation assuming a storativity value of $2x10^{-4}$ (Allen et al., 1997) and water that has been pumped for a period of 20 minutes. Radius of influence range from 50 to 165 m, although the FLASH program is strongly insensitive to r_0 since this parameter appears inside the logarithm of equation (2).

[2] Ambient flow in Ellergill Bridge and Pallaflat Reservoir is close to the nominal detection limit of the flow meter (10m/s).

conditions, and the overall well pumping test transmissivity T. The proportion of the total inflow is given by the change in vertical flow velocity between the top and bottom of layer i, divided by the maximum flow velocity i.e. that above the highest permeable zone, v_{max}, i.e,

$$\frac{T_i}{T} = \frac{\Delta v_i}{v_{max}} \quad (3)$$

Layer hydraulic conductivity k_i is then determined according to equation (1). This method essentially neglects ambient head difference between the layers as a source of vertical flow within the well, whereas the Day-Lewis et al. (2011) methodology accounts for this.

4. Results and discussion

4.1 Aquifer heterogeneities

The optical televiewer logs acquired from the six wells confirm that the characteristics of the St Bees Sandstone aquifer observed in outcrop are also present in the subsurface. The principal heterogeneities are represented by thin mudstone (0.01 to 0.65 m) and white silty sandstone (0.01 to 0.50 m) interbeds in red sandstone, and also by bedding plane fractures, vertical joints and brittle cataclastic faults (Figs. 2, 3 a-c, 4). Vertical joints form a stratabound system in the St Bees Sandstone aquifer since they stop at bed-parallel fractures and sedimentary heterogeneities.

Bedding planes observed both at outcrop along the South Head cliff (Fig. 2 a), and in four of the six logged wells (Black Ling, Bridge End Trial, Ellergill Bridge, Rottington Trial) dip towards the SW at 5º to 20º (mean vector dip azimuth = 228°; mean vector dip angle = 12°; vector magnitude = 0.99; n = 439). By contrast, in the two remaining wells (Thornhill, Pallaflat Reservoir) bedding planes dip towards SE at 5º to 15º (mean vector dip azimuth = 150°; mean vector dip angle = 7°; vector magnitude = 0.98; n = 192).

The Black Ling and Pallaflat Reservoir wells penetrate fault zones, as shown in the geological map (Fig, 1b). Normal faults are well exposed along the South Head Cliff and show development of open fractures, although granulation seams are also present in the damage zones (Fig. 2b). For these wells, the optical logs (Fig. 3c)

show zones which are characterized by a cataclasite with brittle open fractures. Such features represent the typical fault core (*sensu* Caine et al., 1996) in the study area according to Gutmanis et al. (1998) and Nirex (1997). However, although situated on a fault trace, the Ellergill Bridge well apparently cuts only the external part of the fault damage zone, as shown by sub-vertical granulation seams (Fig. 3d). Indeed, granulation seams dominate the external parts of fault damage zones more widely in the study area (Gutmanis et al., 1998). Fault-related and principal bedding plane fractures that are imaged in optical televiewer logs are altered by groundwater flow. These fractures possess small cavities, which act to enlarge tectonic discontinuities (Fig. 3b, c, e). Additionally, some other fractures (Fig. 3f) are partially filled by calcite, which represents the soluble cement of the St Bees Sandstone aquifer (Milodowski et al., 1998; Strong et al., 1994). The wells that intersect faults confirm the observation of Gutmanis et al. (1998): cataclastic fault cores with open fractures and granulation seams occur in the fault damage zone.

4.1.1 *Sedimentary heterogeneities*

The sedimentary heterogeneities of the St Bees Sandstone aquifer have been recognized by integrating optical televiewer and wireline logs (Fig. 4). The results of the geophysical characterization are summarized in stereonet plots with regards to the orientation of both sedimentary and tectonic heterogeneities (Fig. 5). Additionally, the vertical occurrence of these structures is summarized in Table 2.

Sedimentary heterogeneities (Fig. 4) are represented by thin white sandstones (91%) and thin mudstones (9%), typically red in colour. The white sandstone (Fig. 4, feature 1) is characterized by low neutron porosity (14 to 18%) and resistivity (50 to 80 Ω·m), and high values of gamma-gamma density (2.4 to 2.6 g/cm^3) and natural gamma (70 to 100 CPS). The mudstones (Fig. 4, feature 2) are also characterized by low porosity (10 to 18%) and resistivity (40 to 70 Ω·m), and high values of gamma-gamma density (2.4 to 2.55 g/cm^3) and natural gamma (80 to 110 CPS). Despite this, mudstone beds (Hm) can be easily distinguished from the white sandstones (Hws) using the optical televiewer log data, since the former are distinctly red in colour (Figs. 3b and 4). Mudstone beds (Hm) occur with a lower frequency than the white sandstone beds (Hws); average vertical spacing is 16.1 m and individual beds are 0.01 to 0.65 m thick (mean = 0.10 m; σ = 9.91 m; n = 28). In contrast, white sandstone beds are 0.01 to 0.50 m thick (mean = 0.04 m; σ = 5.88 m;

n = 279); they show an average spacing in the boreholes of 2.1 m. Mudstone (Hm) and white sandstone (Hws) beds together are both characterized by finer grain size (silt, fine sand), lower porosity (10 to 18%) and high natural gamma (>70 CPS) values which represent typical petro-lithological characteristics associated with clay mineral and mica bearing units (Bloomfield et al., 2006; Hurst, 2000; Rider, 2000; Yang and Aplin, 2007). Petrological studies on the sedimentary heterogeneities of the St Bees Sandstone Formation confirm the presence of fine-grained clay and mica enriched horizons (Strong et al., 1994).

Units enriched in clay minerals represent partial barriers to the fluid flow in matrix-flow aquifer types (Tellam and Barker, 2006) and typically impede movement of high-density contaminants (e.g., DNAPL) moving towards the bottom of the phreatic zone (Conrad et al., 2002; Lawrence et al., 2006; Oostrom et al., 1999). Furthermore, in the Sherwood Sandstone Group of NE England, mudstone and fine-grained sandstone layers represent thin lower aquicludes for seasonal perched aquifers in the vadose zone (West and Truss, 2006).

4.1.2 *Fractures*

Tectonic features recognized in the optical televiewer and wireline logs include vertical joints, fault related-open fractures and granulation seams. Bedding plane and cross-bedding plane fractures detected by televiewer and wireline logs are typically related to the mechanical reactivation of sedimentary structures in response to a lithospheric uplift or gentle folding of a layered stratigraphic succession (Allen., 1998; Ameen, 1996; Odling et al., 1999; Odonne et al., 2007). Hence, these low-angle inclined fractures must be considered tectono-sedimentary heterogeneities. Calliper logs show diameter increases of the borehole in correspondence with bedding plane fractures (S1) ranging from 1% to 20%, and up to 66% where brittle cataclastic faults are present.

All six studied wells are vertical. Eighty-two per cent of fractures possess inclinations less than 35º. As a consequence, moderate-angle inclination (35º to 60º) characterizes only the 7% of fractures, whereas high-angle to vertical inclinations (60º to 90º) characterize 11% of the fractures. However, note that moderate and high angle inclined fractures are under-sampled in vertical boreholes. The Terzaghi (1965) Correction was applied in contouring to remove bias due to the vertical orientation of the borehole (Fig. 5a). Discontinuities (Fig. 5) have been grouped into

seven different sets (S1, S2, S3, S4, S5, S6, S7). Set 1 (S1) is represented by large bedding plane fractures which gently dip (1º to 20º) both towards SW and SSE. Set 2 (S2) always dips towards NNW (20º to 35º), which is the typical orientation of the cross-bedding in the study area (Jones and Ambrose, 1994; Medici et al., 2015) and likely represents the mechanical reutilization of such discontinuities. Sets S3, S4, S5, S6 are high-angle (65º to 90º) stratabound joints, which terminate where they intersect sub-horizontal discontinuities (Fig. 2). Sets S3 and S4 are NW-SE striking and dip towards NE and SW, respectively; Sets S5 and S6 also represent high-angle stratabound joints and respectively dip towards NW and SW (Fig. 5 c, d). However, fractures of Set 7 (S7) are randomly oriented and show dip angles that vary from 40º to 65º. Such discontinuities (S7) are likely either fault related or caused by drilling.

Vector mean statistics (Fig. 5 c, d) confirm that the four sets of inclined fractures (S3, S4, S5, S6) are related to the stratabound fracturing system since they are characterized by two orthogonal systematic orientations (Gillespie et al., 2001; Odling et al., 1999; Odonne et al., 2007; Rustichelli et al. 2013, 2016).

Mean vectors (Fig. 5) of sedimentary heterogeneities consisting of mudstones and thin white sandstones (Hws, Hm) and bedding plane fractures (S1) show how such sub-horizontal structures possess similar orientations. Evident superimposition of poles to planes in stereoplots confirms how S1 structures are closely related to these sedimentary heterogeneities. Indeed, bedding-plane fractures (S1) represent the mechanical reactivation of the main erosive bounding surfaces and minor planar laminations, which have themselves been the object of previous sedimentological studies (e.g., Jones and Ambrose, 1994; Medici et al., 2015).

Evidence of the mechanical reutilization of erosive bounding surface in the St Bees Sandstone aquifer is related to the fact that the average vertical spacing of S1 fractures in boreholes (1.2 m) matches the average vertical spacing of the 3rd order erosive bounding (*sensu* Miall, 2006) described by Medici et al. (2015) and Nirex (1997) in the study area.

In contrast to the wells which intersect predominantly mainly sub-horizontal features (82%), the scanline surveys have been performed to characterize the multi-layered sub-vertical stratabound-type joints (S3, S4, S5, S6). Stratabound joints represent 75% of the recorded discontinuities; bedding parallel (S1) and cross-bedding (S2) fractures account for the 25% of the total. These low angle inclined fractures (S1, S2) represent minor fissures (length in vertical face = 0.1 - 1m; spacing = 0.2-8.2 m)

which are confined, as the sub-vertical joints, within the major plane beds (Fig. 2a; Tab.2).

These structural surveys confirm that two orthogonal sets of bed-perpendicular joints are present in the studied sandstone (Fig. 6a). The two joint sets strike NNW-SSE and ENE-WSW as in the water wells (Fig. 5). Additionally, the horizontal spacing of the sub-vertical joints ranges from 1.1 m to 1.9 m. This spacing range matches closely with the thickness of the mechanical bedding layers (1.3 to 1.9 m) which vertically limit the joints (Tab. 3). Consequently, the two sets of stratabound orthogonal joints fracture the aquifer into blocks that approximate a cubic shape with an average length of 1.5 m for each face (Fig. 6b).

Only 8% of fractures seen in the cliffs are filled by clay. Additionally, fracture aperture seen in the cliff exposures ranges from 1 mm to 20 mm, but is likely enhanced by the unconfined free face and these values are, hence, likely to be unrepresentative of the aquifer properties at depth (Jiang et al., 2009, 2010; Kana et al., 2013). Vertical joints are visibly persistent in plant view up to 15 m, although exposure is limited along the cliffs at South Head. Moreover, outcrops along the intertidal zone at South Head and Saltom Bay cliffs (Fig. 1) show how NNW-SSE striking joints (S3, S4) are horizontally more extended than ENE-WSW striking joints (S5, S6). Indeed, sets S3 and S4 also occur with a higher frequency than sets S5 and S6 in boreholes (Tab.2).

The fracture system that characterizes the St Bees Sandstone aquifer away from faults shows typical characteristics of a stratabound system. This pattern of fractures is common worldwide to any layered aquifer that has experienced lithospheric uplift (e.g., Billi, 2005; Gillespie et al., 2001; Korneva et al., 2014; Odonne et al., 2007). Indeed, orthogonal sets of vertical joints, which terminate at their point of intersection with bedding planes, represent tectonic features which characterize the Sherwood Sandstone aquifer all across the UK. These features have been related to Cenozoic uplift events (Allen et al., 1998; Carminati et al., 2009; Chadwick, 1997; Hillis et al., 2008; Hitchmough et al., 2007; Wealthall et al., 2001).

4.2 Pumping test analyses

Single-borehole pumping tests conducted previously to this study (Fig. 7a, b, c) have been re-analysed for the six wells that were subject to flow velocity logging, to identify their overall transmissivity to allow quantitative flow-log analysis. Transmissivity values are summarized in Table 4 and range from 35 to 910 m^2/day.

Using Eden and Hazel and Theis solutions it is not possible to calculate the storage coefficient of aquifers from single-well tests (Butler, 1990; Sethi, 2011). Single-well step-drawdown tests should constitute at least 4 steps and data here meet these criteria (Fig. 7a, b). These well step-drawdown tests (Fig. 7a, b; Tabs. 4, S1) have been analysed using Eden and Hazel (1973) which, except for Ellergill Bridge[3], fit the validity conditions suggested by Mathias et al. (2008, 2010) specifically in fractured aquifer-types. These authors show how step-drawdown tests are generally appropriate for the calculation of aquifer parameters where final step flow rates are greater than 350 m^3/day. Alternatively, step-drawdown tests characterized by lower flow rates (<350 m^3/day) but with a step duration of less than 60 minutes also reproduce reliable aquifer parameters. Our step-drawdown curves show optimum fits since residual mean (0.01-0.15 m^2/day) and residual standard deviation (0.16-0.80 m^2/day) are characterized by significant lower values compared to transmissivities (41-913 m^2/day). Misfits between experimental data and model curves occur only in Bridge End Trial at late pumping stages; this likely arises from partial leakage from the overlying glacial cover (Figs. 7b, S1).

Recovery phases of the step-tests and those of the tests of longer duration at constant flow rate (Fig. 7b) have also been analysed, following Theis (1935). This methodology determines transmissivity from single borehole tests assuming non-steady state horizontal flow.

A comparison of the transmissivity values calculated using all the available datasets (Tab. 4) indicates that recovery phase Theis analysis of step-tests yields transmissivity values 14 to 24% lower than the Eden and Hazel (1973) analysis of the drawdown phase. This systematic difference in transmissivity between step-drawdowns and relative recovery may be related to the fact that well loss correction is neglected in the Theis recovery analysis, and this method consequently underestimates transmissivity (Clark, 1977). However, Theis recovery analysis of the longer constant rate tests produced transmissivity values both higher and lower than the Eden and Hazel analyses of step tests (Tab.4). These differences probably arise due to the different test durations and hence volume investigated which resulted in a lack of well loss correction in some wells (Le Borgne et al., 2004; Le Borgne et al.,

[3] Ellergill Bridge represents the only drawdown well test which does not meet the validity conditions demonstrated by Mathias et al. (2008; 2010). To address this issue, the 5th step test of duration > 60 minutes has been neglected in calculating transmissivity, which itself yields reliable values close to other well tests analysed for this borehole (Tab.4).

2006a; Le Borgne 2006b; Neuman and Di Federico, 2003; Noushabadi et al., 2011). Given both the wide range in durations and investigated volumes associated with the recovery of constant rate tests, and the neglection of well loss in all the available recovery datasets, transmissivities derived from the Eden and Hazel approach have been used here for flow-logging analysis. These drawdown step tests show how aquifer transmissivities range from 41 up to 99 m^2/day for five of the six flow-logged wells. Only Thornhill Trial shows a significantly higher transmissivity value (913 m^3/day); this well seems to be influenced by the River Ehen which represents the principal river in the Sellafield plain and is only 100 m distant (British Geological Survey, 2015; Meritt and Auton, 2000). Black Ling (66 m^2/day) and Pallaflat Resevoir (99 m^2/day) are the only wells drilled in correspondence of mapped fault traces on the geological map (Fig 1b, Tab. 1); these show transmissivities at the upper end and in the middle of the range 41 up to 99 m^2/day respectively top (Tab. 4).

4.3 Upscaling hydraulic conductivity

Available transmissivity values from pumping tests for the six studied boreholes (Tab. 4) are compared with the screen transmissivity which is obtained from the upscaling of cored hydraulic conductivity values available for the St Bees Sandstone aquifer. These plug-scale hydraulic conductivities show similar ranges across the Egremont-Sellafield area (Fig. 1). In fact, hydraulic conductivity from cored plugs range from 8.3×10^{-6} up to 1.2 m/day and from 4.2×10^{-6} up to 0.8 m/day for the Egremont and Sellafield area, respectively (Allen, 1997; Nirex, 1992a, 1992c, 1993b, 1993c). Thus, these values have been grouped together in order to upscale screen transmissivity in the six studied boreholes aiming to maximise sample representability. The horizontal hydraulic conductivity (K_h) from sandstone plugs have been upscaled since it represents preferential flow direction in a layered aquifer which is characterized by sub-horizontal beds (dip angle = 5º-20º; mean vector = 10º; n = 631) and sandstone represents 95% of thickness penetrated in the six bereholes. The K_h geometric mean of sandstone plugs (n = 177) is 1.3×10^{-2} m/day. This average values has been multiplied by the screen length (see Tab. 1) to compute upscaled geometric and harmonic transmissivities in each flow-logged borehole (Tab. 4).

The screen transmissivities which are obtained by the upscaling of K_h geometric mean show values ~10^2 lower than transmissivity from well tests ($T_{well\ test}/T_{harmonic}$ =

35-653; arithmetic mean = 153; σ = 224). Thus, well tests transmissivity values are significantly higher than those implied for the matrix by upscaling, suggesting that fractures dominate during pumping tests.

4.4. Fluid logs

The FLASH program for flow log analysis (Day-Lewis et al., 2011) is suitable both for aquifers dominated by matrix and fracture flow and is commonly used in the analysis of sandstone aquifers (e.g., Gellasch et al., 2013; Lo et al., 2014). Here the program was used for analysing flow velocity profiles of shallow boreholes in “fracture mode” instead of “layer mode”, since the water flow in the shallow aquifer tested here is dominated by fractures. Indeed, flow velocity profiles from this study show major changes in correspondence to tectonic discontinuities. Analysis of fluid velocity, temperature and conductivity curves was compared with optical televiewer images aiming to estimate the percentage of flowing fractures. The proportion of flowing fractures was found to be ~10%, which includes fractures that bound flow zones (n=33) in the six studied wells and a clusters of fault-related fractures in the Back Ling and Pallaflat Reservoir wells (n=23).

4.4.1 Fluid logs analysis - stratabound system

Velocity, temperature and conductivity logs carried out in Bridge End Trial, Rottington Trial and Thornhill Trial wells characterize the aquifer away from fault zones according to the geological map (Fig. 1b; Tab. 1). The background information (Nirex, 1997; British Geological Survey, 2015) also does not indicate the presence of fault-related structures near these three wells. Optical televiewer and calliper logs confirm how the fracturing network of these wells is not characterized by fault-related structures i.e. an absence of displaced horizons, cataclasites and intervals characterized by significant diameter variations. Thus, the fracturing pattern is dominated by bedding plane fractures (S1) and vertical joints (S3, S4, S5, S6); cross-bedding (S2) and drilling-induced fractures (S7) also occur. Temperature, conductivity and velocity logs were measured initially in ambient conditions and then under pumped conditions: pumping rates were 132 L/min in Bridge End Trial, 50 L/min in Rottington Trial and 168 L/min in Thornhill Trial. Pumping was maintained at a constant rate for 20 minutes before flow logging using a tool-speed of 10 m/min

(wells were logged both downwards and upwards but the downward flow logs are presented and analysed here, as these have better data quality). Additionally, temperature and fluid conductivity were also logged under ambient and pumped conditions.

The FLASH program has been used to constrain hydraulic conductivity from fluid velocity logs; fluid conductivity, temperature and flow velocity, in both ambient and stressed conditions are reported (Figs. 8 and S2). The modelled parameters which are represented by T_{factor} (ratio between single layer and well test transmissivity, T_i/T), Δh_i (difference in head between the well and the far-field for each layer) and the hydraulic conductivity for each layer (k_i), are summarized in Table 5. Interpretations of flow velocity log profiles (Fig. 8) are based on the selection of marked changes of the fluid flow velocity, which divides the open well section into hydraulic layers (Figs 8 and 9). Six layers (L1-6) were modelled for Bridge End Trial; Thornhill Trial and Rottington Trial were modelled using eight layers (L1-8). Typically layer boundaries identified in this way corresponded to bedding plane fractures (S1) seen in the optical televiewer logs. Some layer boundaries are marked by sharp changes of flow velocity, which then remains substantially constant within the zone. Such layers include L2 and L3 in Thornhill Trial, L3 and L5 in Bridge End Trial and L5 in Rottington Trial. Thus, these layers are internally impermeable and only the sub-horizontal fractures at their boundaries conduct flow into the well. Flow velocity (Fig. 8) in other modelled layers is characterized by a basal change and then by a constant slope within the layer (e.g. L5 in Thornhill Trial). This means that other permeable structures contribute to the flow within these layers. Indeed, the optical televiewer and calliper logs indicate the presence of minor fractures characterized by further bed-plane (S1), cross-bed (S2) discontinuities, stratabound joints (S3, S4, S5, S6) and rare non-natural fractures (S7) within such layers.

Layer hydraulic conductivity values from the wells that are not close to fault traces typically range from 0.1 to 4.6 m/day (Tabs. 5, S2), although values higher than 5 m/day occur where a layer is bounded by prominent bed-parallel fractures. These S1 discontinuities are characterized, according to the calliper log, by up to 20% borehole diameter enlargement. Thornhill Trial (Fig. 8a) and Rottington Trial (Fig. S2) wells are characterized by both inflow and outflow horizons. Inflows occur in the lower part of the Thornhill Trial borehole (Fig. 8a) and are associated with marked changes in both water resistivity and temperature; the upper parts of these wells are characterized by

outflows (seen as reducing upward ambient flow near the top of the open section). By contrast, Bridge End Trial (Fig. 8b) is artesian and hence overflowed throughout logging; it is thus characterized only by inflows. Note that the lack of variation of conductivity and temperature at the outflow horizons identified in Figure 8a is expected, since there is no contribution of water flowing from different compartmentalized levels. Bedding plane fractures have been found in this analysis to be important flow pathways both in ambient and stressed conditions. Alteration (detected by the optical televiewer) acts to enlarge these permeable fractures (K>5 m/day) that may transport contaminants in groundwater at high flow velocities. Barker et al. (1998) found using tracer tests in the Sherwood Sandstone Group in the Cheshire Basin flow velocities up to 140 m/day which are typical of carbonate karst aquifers suggesting how enlarged fractures may transport contaminants at velocities which are unexpected for a siliciclastic porous aquifer.

Flow-logging analyses undertaken in other lithified and fractured sandstone aquifers (Gellash et al., 2013; Lo et al., 2014; Runkel et al., 2006) away from fault zones show similar results, which are represented by significant velocity variation in correspondence of large bedding fractures which bound the modelled flow zones. Additionally, Morin et al. (1997) in the Passaic Sandstone in New Jersey and Bouch et al. (2006) in the Sherwood Sandstone aquifer of the Cheshire Basin found low proportion (<20%) of fractures with measurable flow using borehole flow-logging similarly to this work (where the proportion was approximately 10%). Hitchmough et al. (2007) also pointed out the importance of bedding-parallel fractures on conducting water flow in the Sherwood Sandstone aquifer in the Cheshire Basin at relatively shallow depths (≤ 180 m). These authors found analysing fluid-logs that 9% of fractures produced detectable flow, similar to our hydrogeophysical study.

Flowing low-angle inclined fractures (<25°), as seen in our study of the St Bees Sandstone Formation, are also common for non-faulted wells in fractured limestone, dolostone and gneiss subjected to flow logging (e.g., Le Borgne et al., 2006a; Paillet, 1998, 2004), these include fractures along sub-horizontal foliations in gneiss and bedding discontinuities in carbonate rocks.

4.4.2 Fluid logs analysis - fault zones

Flow velocity, temperature and conductivity logs have also been carried out in three of the six wells which have been drilled close to fault traces (Fig. 1; Tab. 1), to

characterize the impact of fault zones on flow. Flow logging was performed under ambient and pumped conditions, as previously described for the non-faulted wells: pumping rates were 150 L/min in Black Ling, 156 L/min in Ellergill Bridge and 126 L/min in Pallaflat Reservoir (Fig. 1b).

Background information (British Geological Survey, 2015; Nirex, 1997) indicates the presence of extensional faults in correspondence of Black Ling, Ellergill Bridge and Pallaflat Reservoir wells (Fig. 1b; Tab. 1). Optical televiewer and calliper logs confirm how the fracturing network of these wells is affected by fault-related structures such as cataclasites, open fractures and granulation seams. Indeed, optical televiewer logs show fault cataclasites (Figs. 3d and 9a) in Black Ling well between 16 and 22 mASL, and also at the bottom of the well which is collapsed due to the presence of a major cataclastic fault structure. Pallaflat Reservoir (Fig. 9a) well is also affected by faulting between 10 and 14 mASL. However, Ellergill Bridge well cuts only the external part of a fault zone so it does not show cataclasites. In this well vertical granulation seams are detected by the optical televiewer log. Bedding plane fractures (S1), cross-bed fractures and vertical joints (S3, S4, S5, S6), which characterize the entire aquifer, complete the fracturing pattern in these three faulted wells.

Calliper logs indicate enlargement of the well diameter in correspondence of fault cataclasites by up to 66%, 54% and 30% in the Black Ling, Ellergill Bridge and Pallaflat Reservoir wells, respectively. By contrast, in boreholes that are not characterized by faulting, the well diameter does not increase more than 20% in correspondence to major bedding plane discontinuities.

Velocity flow logs in these three wells (Black Ling, Ellergill Bridge, Pallaflat Reservoir; Fig. 9) have been complicated by problems related to water turbulence due to variations in borehole diameter or low ambient flow rates (0-18 mm/s) close to the nominal detection limit of the flow meter (Day-Lewis et al. 2011; Grass, 1971; Tsang et al., 1990; Paillet 2004). Consequently, fitting experimental flow profiles in Ellergill Bridge and Pallaflat Reservoir wells using the FLASH program proved problematic, although a fit was obtained for Black Ling well (Fig. 9a). The interpretation of the Black Ling flow velocity profile uses four flow zones; the upper flow zone includes a section showing fault cataclasites near the top of the well, which does not cause any inflow or outflow. Notably, temperature and conductivity logs also do not show any anomaly in correspondence of this feature. However, a major cataclastic fault is

present at the bottom of the logged interval (Fig. 9a) and a collapse is present directly below the end of logged interval; these zones contribute 50% of flow into the Black Ling well; analysis indicates a hydraulic conductivity of 5.2 m/day (L1, Tab. 6).
Pallaflat Reservoir well (Fig. 9b) shows cataclasites between 10 and 14 mASL that produces 47% of the flow; analysis indicates a hydraulic conductivity of 7.4 m/day (L3, Tab. 6). Despite the different methodologies used to quantify the water flow, in both cases cataclasites characterize about the 50% of the flow in a single-well test. However, the other 50% of the flow in both Pallaflat Reservoir and Black Ling wells derives from large bedding plane fractures (S1), which represent further important flowing discontinuities.
Ellergill Bridge well (Fig. 9c; Tab 6) cuts the external part of a fault damage zone and does not appear to cross-cut the fault core; no cataclasites or fractures showing displacement, are observed. Consequently, flow in this borehole is dominated by bedding -plane fractures. Indeed, 42% of the transmissivity is related to the L2 zone, which represents a cluster of S1 fractures. The upper zone above this characterizes the remaining 58% of the transmissivity. Ellergill Bridge well shows hydraulic behaviour similar to the non-faulted wells that have been previously described (Bridge End Trial, Rottington Trial, Thornhill Trial). All these flow-logged boreholes are characterized by major single bedding fractures, as well as clusters of minor bedding fractures, which give flow zones with hydraulic conductivity higher than 5 m/day. Consequently, bedding fractures (S1) can produce hydraulic conductivities comparable to cataclasite flow zones.
Previous application of flow logging in faulted zones in crystalline rocks (e.g., Davison and Kozak, 1988; Le Borgne et al., 2006a; Martin et al., 1990; Roques et al., 2014) show similar result to the St Bees Sandstone aquifer, in that flow is dominated both by fault-related features and also by sub-horizontal, bedding-related discontinuities, with no contribution from the rock matrix evident.

4.5 Sherwood Sandstone aquifer

The hydro-geophysical characterization of the shallow Bees Sandstone aquifer (≤180 m) of the East Irish Sea Basin is compared in this work with both (i) the deep St Bees Sandstone aquifer (180 to 400 m subsurface depth) undertaken as part of the investigation for the Sellafield nuclear waste repository; and (ii) the Sherwood Sandstone aquifer of the Cheshire Basin which was previously investigated by

crossing borehole logging, packer and intergranular permeabilities tests (Allen et al., 1997; Brassington and Walthall, 1985).

The comparison between the hydro-geophysical characterization undertaken in this work with that of the deeper St Bees Sandstone aquifer (Streetly et al., 2000) aims to provide an improved understanding of the mechanisms that reduce both permeability and contaminant transport velocities at increasing depths in a strongly lithified sandstone aquifer-type. Our results are also compared with those from previous studies of the Sherwood Sandstone aquifer of the northern Cheshire Basin, where analogous succession are also fractured and layered but less mechanically resistant, and characterized by higher matrix porosity and hydraulic conductivity values (Allen et al., 1997; Daw et al., 1974; Yates, 1992). Furthermore, normal faults in the northern Cheshire Basin have been the object of hydrogeological studies from the mid 1800s to present (Griffiths et al., 2016; Mohamed and Worden, 2006; Moore, 1902; Morton, 1870; Saymour et al., 2006; Tellam, 2004), which allows comparison of their hydraulic behaviour with those in the St Bees Sandstone aquifer (West Cumbria, East Irish Sea Basin).

4.5.1 Review of pumping tests in the St Bees Sandstone aquifer.

Pumping test transmissivity (Fig. 10) values from the six studied wells in the West Cumbrian region have been integrated with all the available hydraulic tests that have previously been realised in the St Bees Sandstone aquifer (Allen et al., 1997; Streetly et al., 2000). Additionally, all the information concerning both transmissivity values and test parameters has been summarized in Table 7. Transmissivity values of the shallow part of the St Bees Sandstone aquifer have been plotted in a single box plot (box plot A, Fig. 10), which collates hydraulic test data from both the West Cumbria and Carlisle areas. These values have been grouped together because the aquifer is characterized by the same lithological features and intergranular permeability (Allen et al., 1997; Brookfield, 2004, 2008; Jones and Ambrose, 1994; Medici et al., 2015; Nirex, 1992a, 1992c, 1993b, 1993c) across these areas. However, all the transmissivity values obtained during the hydrogeological investigation of the more deeply buried St Bees Sandstone aquifer in Sellafield (Streetly et al., 2000) have been plotted in a separate box plot (box plot B, Fig. 10).

The two groups of hydraulic tests show a systematic difference of two orders of magnitude (10^2) between each pair of statistical parameters (maximum, minimum,

25th percentile, 75th percentile, geometric and harmonic means). The two groups of hydraulic tests are characterized by similar screen length and borehole diameter ranges (Tab. 7). Although the two groups differ in flow rates and test duration with generally lower flow rates and longer test durations for the Sellafield group, this is likely to be simply a consequence of the lower transmissivities seen here. In fact, only low extraction rates were achievable, and a longer test duration was needed to produce a measurable response. Additionally, although the two groups of pumping tests differ for flow rates and test duration; these two physical parameters show wide ranges of values which are reported in Table 7. Consequently, there is always partial superimposition with regards to flow rates and pumping duration comparing pumping tests in the shallow and the deep St Bees Sandstone aquifer.

Matrix permeability values from cored plugs show similar values for the shallow and deep St Bees Sandstone aquifer. In fact, plug-scale hydraulic conductivity ranges are 8.3×10^{-6} - 1.2 m/day and 4.2×10^{-6} - 0.8 m/day for the shallow and the deep aquifer, respectively (Allen, 1997; Nirex, 1992a, 1992c, 1993b, 1993c). Additionally, according to Black and Brightman (1996), the chemical composition of groundwater in the shallow and the deep St Bees Sandstone aquifer are largely the same as indicated by the comparison of groundwater chemistry and conductivity. A Westbay multi level monitoring system, which has been installed as part of the planning of the Sellafield nuclear repository, shows how groundwater salinity strongly increases in the Sellafield area only below the lower boundary of the St Bees Sandstone Formation (Black and Brightman, 1996). Given these similarities between the shallow versus deep aquifer, the observed differences in transmissivity are most likely to result from higher fracture permeabilities which localize inflow and outflow horizons at depths shallower than 180 m (Fig. 11a). Hydraulic head measurements which have been realised by the same Westbay monitoring system that was used for fluid conductivity measurements also shows how the aquifer is characterized by a horizontal hydraulic gradient which is essentially constant with depth (Black and Brightman, 1996). Additionally, the St Bees Sandstone aquifer is ~ 100 times more transmissive in its shallow part than buried below 180 m (Streetly et al., 2000). Thus the shallow St Bees Sandstone aquifer must be characterized by higher groundwater flow rates which will act further to enhance alteration of fractures. The relatively high permeability of fractures in the shallow part of the aquifer (≤ 180 m) may be related either to fracture closing with increasing depth, or to alteration of fractures as is

typical in the shallow part of sandstone aquifers (Fig. 11 a; Jiang et al., 2009, 2010; Wray, 1997). Calcite represents the soluble cement in the St Bees Sandstone aquifer (Milodowski et al., 1998; Strong et al., 1994) and evidence of elevated groundwater flow enhancing dissolution of this mineral along fractures is provided by borehole optical televiewer images showing partially mineralized fractures (Fig. 3f). Furthermore, optical televiewer logs also indicate the occurrence of small cavities that enlarge tectonic fractures (Fig. 3b, c, e) such as bedding plane (S1) and fault-related (S7) fractures; these may also be a result of calcite dissolution.

The highly permeable shallow aquifer shows a developed fracturing network, which is characterized by flowing open fractures (Fig. 11a; faults, bedding fractures). These tectonic fractures are capable to conduit fluid flow at low confining pressure (<5 MPa), but their permeability reduces at higher pressures, as demonstrated by multistage permeability tests based on analysis of plugs of the St Bees Sandstone Formation (Daw et al., 1974).

The deep St Bees Sandstone aquifer, is also characterized by a reduction of transmissivities (25%) occurring in association with mudstone units (Streetly et al., 2000). This lower transmissivity in the mudstone-rich basal sedimentary sequence may be related to one or more of the following: (i) flow through the low-permeability mudstones characterizing the basal stratigraphy in a matrix-flow aquifer (Alexander et al., 1987); (ii) further reduction of fracture aperture due to the lithostatic load (Jiang et al., 2009, 2010); or (iii) less development of fracturing due to stress release on the plastic mudstone-beds (Reks and Grey, 1982). Matrix flow as principal flow driver in the deep St Bees Sandstone aquifer is supported by the first derivative of recovery tests undertaken by Streetly et al. (2000). In fact, these curves show no multiple plateaus which characterize first derivatives in double-porosity media (Dewandel et al., 2011; Odling et al., 2013; van Tonder et al., 2001; Zhang et al., 2000). Additionally, well test transmissivity values in the deep St Bees Sandstone aquifer (Streetly et al., 2000; see bottom line of Tab. 7) better match our upscaled transmissivity values derived from plug-scale hydraulic conductivity (see Tab. 4) indicating that pores are the main flowpaths in the deeper aquifer. Thus, the transmissivity reduction (25%) in the lower sedimentary sequence must be related to flow through the low permeability mudstones which characterize the base of the sedimentary sequence. However, fracture flow may remain significant in the presence of faults, since well tests on the deep aquifer undertaken with packers in

the vicinity of normal faults show relatively high transmissivity values (Fig. 11b; Nirex, 1992b, 1993a; Streetly et al., 2000).

4.5.2 *Comparison with Sherwood Sandstone aquifer in the Cheshire Basin*

The Sherwood Sandstone Group in the northern Cheshire Basin (Fig.1) has been object of several hydrogeological studies which includes packer, pumping tests, intergranular permeability and tracer tests (Allen et al., 1997; Barker et al., 1998; Brassington and Walthall, 1985).

The lowermost part of this group is represented by the Chester Pebble Beds Formation, which is dominated by a coarse to medium grained pebbly sandstone of fluvial origin. The overlying Wilmslow and Helsby Sandstone formations are characterised by a weak, fine-grained sandstone of aeolian and fluvial origin (Mohamed and Worden, 2006; Mountney and Thompson, 2002). Overall the Sherwood Sandstone Group of the Cheshire Basin is mechanically less resistant (overconsolidated sand to weak rock), and is characterized by higher porosity (interquartile range = 21.6-26.5%) and lower hydraulic conductivity (interquartile range = 0.08-1.5 m/day) values compared to the West Cumbrian St Bees Sandstone aquifer (Allen, 1997; Bell, 1992; Daw et al., 1974; Yates, 1992).

Brassington and Welthall (1985) have undertaken packer and pumping tests at relatively shallow depths (≤ 130 m) in the Sherwood Sandstone aquifer of the Cheshire Basin comparing them with the upscaling of the hydraulic conductivities from cored plugs. Plugs for hydraulic conductivity measurements were from the same borehole and well logging did not show presence of fault structures.

The findings of the work undertaken by Brassington and Welthall (1985) in the Sherwood Sandstone of the Cheshire Basin contrasts with the upscaling of the hydraulic conductivity realised for the shallow St Bees Sandstone aquifer in this work. The authors found that, as for the shallow St Bees Sandstone aquifer, the upscaled screen transmissivity remains lower than the field test transmissivity. However, the ratio between plug and field scale T was less than 10 ($T_{Well\ test}/T_{Screen}$ = 1.9-6.9), which contrasts with the larger ratios seen here for the St Bees Sandstone aquifer (~ 10^2).

Packer and fluid-logs tests also show how the difference between plug and field scale values resulted from a few (3-4 per each borehole) flowing bedding plane fractures. By contrast, there is a good match between T values from the two studied

scales (plug and field scale) in the remaining part of the borehole. This hydraulic behaviour is common to other sandstone aquifers worldwide in non-faulted areas. In fact, flow in well tests in the Penrith (NW England) and in the Cambrian Sandstone (North America) aquifers is characterized both by intergranular porosity and large bedding-parallel fractures (Gellash et al., 2013; Price et al., 1982). The St Bees Sandstone aquifer at relatively shallow depth (≤ 180 m) is also characterized by major flowing bedding fractures with hydraulic conductivity higher than 5 m/day. However, flow in the St Bees Sandstone aquifer not in correspondence with major bedding fractures seems to be dominated by fissures as associated with minor cross-bedding and sub-vertical (stratabound joints) fractures. The fact that the upscaling of plug-scale hydraulic conductivity showed such a large difference with respect to the well tests (~10^2) effectively excludes matrix as significant flow contributor during pumping.

Hydraulic conductivity profiles from packer tests in deep boreholes (230 up to 450 m deep) that penetrate the Sherwood Sandstone aquifer in the Meseyside area (Cheshire Basin) show a reduction in permeability below 150 m similarly to our study in West Cumbria (Allen et al., 1997; Brassington and Walthall, 1985). Tracer tests undertaken by Barker et al. (1998) show a karst-like flow velocity (140 m/day) in the shallow Sherwood Sandstone aquifer of Merseyside. Alteration along fractures in the shallow Sherwood Sandstone aquifer (≤ 180 m) has been detected in this work by the optical televiewer which confirms how groundwater alteration plays a key role on creating a high permeability zone. Thus, the Sherwood Sandstone aquifer in West Cumbria as well as in Merseyside shows a permeable shallow part (≤ 180 m) which is characterized by potential high flow velocity with bedding fractures representing 'karstified' flow-pathways (Allen et al., 1997; Brassington and Walthall, 1985; Barker et al., 1998).

Normal fault zones in the Wilmslow and Helsby Sandstone formations of the Sherwood Sandstone Group in Merseyside appears substantially different with respect to the St Bees Sandstone Formation as they are dominated by granulation seams (Griffiths et al., 2016; Fowles and Burley; 1994). By contrast, fault zones in the St Bees Sandstone Formation of the East Irish Sea Basin are characterized by a higher occurrence of open fractures (Fig. 2b). This different structural style has been related either to the argillaceous matrix of the St Bees Sandstone which allows brittle failure at lower stresses, or to the intense post-Triassic fault reactivation which

produced open-fracture in this strongly lithified sandstone (Knott, 1994; Milodowski et al., 1998). This different structural style seems to affect the fault zone hydraulic characteristics in the Sherwood Sandstone aquifer in West Cumbria and Merseyside. Bedding-parallel fractures cut granulation seams in fault damage zones and water flow seems to be dominated by these sub-horizontal fissures (Fig. 9c, Ellergill Bridge) masking the barrier potential of granulation seams perpendicular to the fault plane. Fault slip planes and open fractures characterize 50% of flow entering boreholes penetrating fault cores (Fig. 9 a, b).

Thus, faults in this lithified sandstone represent primary conduits for fluid flow and show low barrier potential. By contrast, normal faults deforming the Wilsmlow and the Helsby sandstone formations (Cheshire Basin) were recognized as flow-barriers based on the geochemical evidence of limited water mixing between compartmentalized horsts and grabens (Mohamed and Worden, 2006). It has been suggested that barrier behaviour led to K values at the regional scale of only 0.05 m/day perpendicular to the fault plane in the weak-rock Sherwood Sandstone of the Cheshire Basin (Saymour et al., 2006).

5. Conclusions

The hydro-geophysical characterization of the St Bees Sandstone aquifer undertaken in this work has highlighted the presence of a pervasive stratabound fracture network characterizing the sandstone aquifer. These stratabound fractures show two sets of orthogonal vertical joints that stop at their point of intersection with low-angle-inclined bedding parallel fractures. The key sedimentary heterogeneities include thin, low-porosity layers characterized by mudstone and fine-grained sandstone. Collectively, these features form matrix blocks, which may be approximated as cubes with dimensions of 1.5 m length. Normal faults, locally, complicate the fracturing pattern, since further open fractures cutting both stratabound joints and bedding plane fractures occur in fault cores and damage zones.

In the shallow aquifer tested here (≤ 180 m depth), marked temperature, conductivity and flow velocity variations in well-bore fluid logs are localized to bedding parallel fractures and faults, which represent the main borehole inflow and outflow points. Clear indications of the importance of fractures in contributing flow to wells in the shallow aquifer include (i) sharp changes in flow-log fluid velocity in association with

principal fractures, and (ii) stratigraphic intervals up to 15 m thick showing no detectable inflows, suggesting how matrix is a minor contributor to permeability in the shallow (≤180 m depth) part of the aquifer.

Quantitative analysis of well-bore flow logs from the St Bees Sandstone aquifer show that flow zones characterized by hydraulic conductivity higher than 5 m/day typically represent up to 50% of the overall transmissivity, and are represented by the following structures: cataclasite sections where fault planes intersect the wells; single large bedding fractures; and clusters of minor bedding fractures. Specifically, fault-related fracture-corridors dominate the flow in wells which cross-cut cataclastic fault cores, because fault-related fractures establish communication between flowing bedding plane fractures. However, bedding fractures become the principal flow conduits to wells in the external part of fault damage zones or in non-faulted areas. Fluid flow along these bedding plane fractures is likely enhanced by stratabound joints which are undersampled in vertical boreholes.

The St Bees Sandstone aquifer at depths greater than 180 m was the object of a hydro-geophysical characterization as part of the planning of the proposed Sellafield nuclear waste repository in the 1990s. This deep aquifer is characterized by transmissivity values which are two orders of magnitude lower than the St Bees Sandstone aquifer investigated at shallower depths (≤180 m). Since petrophysical properties, water chemistry and hydraulic flow regime are essentially similar to that for the shallow aquifer, the large difference in transmissivity most likely arises from higher fracture permeability at depths shallower than 180 m. Such a difference may arise because fractures are more open at relatively low vertical confining pressure (<5 MPa) in the shallower part of the aquifer. Additionally, tectonic fractures in the shallow aquifer show alteration, as indicated in optical televiewer logs. This probably arises from shallow groundwater flow leading to calcite dissolution along tectonic features. Data from the low transmissivity deep sandstone aquifer (≥180 m depth) show that those stratigraphic units characterized by a higher occurrence of mudstone beds are characterized by relatively lower transmissivity than those dominated by medium-grained channel sandstones. This, coupled with a match between upscaled plug and field-well test scale, suggests that the matrix is a significant contributor to flow at these depths (180 to 400 m). This does not seem to be the case in the shallower aquifer because of the much larger permeability of the

fracture network, which dominates over flow associated with the heterogeneous sedimentary matrix.

The Triassic St Bees Sandstone aquifer in the East Irish Sea Basin represents an example of a mechanically resistant sandstone aquifer-type which is characterized by (i) fluid flow entirely dominated by fractures in its shallow part; and (ii) extensional faults representing significant flow conduits. This contrasts the Sherwood Sandstone aquifer of the Cheshire Basin that mechanically weaker is characterized by water flow supported both by matrix and fractures, and normal faults represent significant flow- barriers.

Acknowledgements

The authors thank Total E&P UK Limited for funding this research project. Well logging was conducted by European Geophysical Services Ltd. The British Geological Survey (Wallingford, UK) and the Environmental Agency (Warrington, UK) provided datasets concerning historical pumping tests. Simon Gebbett (Environment Agency) gave useful logistic advice during preliminary visits to the field site. Vanessa Butterworth (University of Leeds) organized pumping tests data. Philippe Ruelland (Total E&P) is thanked for supporting the project. The results of this research also benefitted from discussions with Antoni Milodowski (British Geological Survey), Noelle Odling (former University of Leeds), Gérard Massonnat (Total E&P) and Phill Merrin (United Utilities) regarding the development of stratabound rock joints, and the hydrogeology of the Sherwood Sandstone aquifer. Frederick Day-Lewis (United States Geological Survey) provided useful instructions and recommendation during flow-log analysis. Finally, this work has benefitted from the constructive review comments from two anonymous reviewers, for which we are grateful.

Supplementary material

The online version of this paper contains fluid composite logs and flow-logging parameters computed with the FLASH program in relation to the Rottington Trial well. Parameters (step test flow rate, formation loss, turbulent head loss, observed vs modelled step-test drawdown) that allowed calculation of aquifer transmissivity using the methodology of Eden and Hazel (1973) are reported in the supplementary on-line material.

References

Akin, S., 2001. Estimation of fracture relative permeabilities from unsteady state core floods. J. Petrol. Sci. Eng. 30 (1), 1-14.

Akhurst, M.C., Barnes, R.P., Chadwick, R.A., Millward, D., Norton, M.G., Maddock, R. H., Kimbell, G.S., Milodowski, A.E., 1998. Structural evolution of the Lake District Boundary Fault Zone in west Cumbria, UK. Proceed. York. Geol. Soc. 52 (2), 139-158.

Alexander, J., Back, J.H., Brightman, M.A. 1987. The role of low-permeability rocks in regional flow. In: Goff, J.C., Williams, B.P.J., (Eds.), Fluid Flow in Sedimentary Basins and Aquifers. Geol. Soc., London, Spec. Publ. 34, p.p. 173-183.

Allen, D.J., Bloomfield, J.P., Gibbs, B.R., Wagstaff, S.J., 1998. Fracturing and the hydrogeology of the Permo-Triassic sandstones in England and Wales, technical report WD/97/34, 1-89. BGS, Nottingham, England (UK).

Allen, D.J., Brewerton, L.M., Coleby, B.R., Gibbs, M.A., Lewis, A.M., MacDonald, S.J., Wagstaff, A.T, Williams, L.J., 1997. The Physical Properties of Major Aquifers in England and Wales. Technical Report WD/97/34, 157-287. BGS, Nottingham, England (UK).

Allimendinger, R.W., Cardozo, N., Fisher, D., 2012. Structural Geology Algorithms: Vectors and Tensors. Cambridge University Press, Cambridge, England (UK).

Ameen, M.S., 1995. Fractography and fracture characterization in the Permo-Triassic sandstones and the Lower Palaeozoic Basement, West Cumbria, UK. In: Ameen, M.S. (Ed.), Fractographic Studies-Fractography Applied to Fracture Analysis in Field Studies Aimed at Understanding Regional Tectonics. Geol. Soc. London, Spec. Publ. 92, pp. 97-147.

Antonellini, M.A., Aydin, A., Pollard, D.D., 1994. Microstructure of deformation bands in porous sandstones at Arches National Park, Utah. J. Struct. Geol. 16 (7), 941-959.

Appleton, P.R., 1993. Probabilistic safety assessment for the transport of radioactive waste to a UK repository at Sellafield. Int. J. Rad. Mat. Trans. 4, (3-4), 205-211.

Avcı, C.B., 1992. Flow occurrence between confined aquifers through improperly plugged boreholes. J. Hydrol. 139 (1), 97-114.

Balsamo, F., Storti. F., 2010. Grain size and permeability evolution of soft-sediment extensional sub-seismic and seismic fault zones in high-porosity sediments from the Crotone basin, southern Apennines, Italy. Mar. Petrol. Geol. 27 (4), 822-837.

Barker, A.P., Newton, R.J., Bottrell, S.H., Tellam, J.H., 1998. Processes affecting groundwater chemistry in a zone of saline intrusion into an urban sandstone aquifer. Appl. Geochem. 13 (6), 735-749.

Barnes, R.P., Ambrose, K., Holliday, D.W., Jones, N.S., 1994. Lithostratigraphic subdivision of the Triassic Sherwood Sandstone Group in west Cumbria. Proceed. York. Geol. Soc. 50 (1), 51-60.

Barrett, M. H., Kevin M.H., Stephen, P., Lerner D.N., Tellam, J.H., French, M.J., 1999. Marker species for identifying urban groundwater recharge sources: a review and case study in Nottingham, UK. Water Resour. 33 (14), 3083-3097.

Bashar, K., Tellam, J.H, 2011. Sandstones of unexpectedly high diffusibility. J. Contam. Hydrol. 122 (1), 40-52.

Bauer, S., Bayer-Raich, M., Holder, T., Kolesar, C., Müller, D., Ptak, T., 2004. Quantification of groundwater contamination in an urban area using integral pumping tests. J. Contam. Hydrol. 75 (3), 183-213.

Beach, A., Welbon, A. I., Brockbank, P. J., McCallum, J. E., 1999. Reservoir damage around faults: outcrop examples from the Suez rift. Petrol. Geosci. 5 (2), 109-116.

Bell, R.G., 1992. The durability of sandstone as building stone, especially in urban environments. Bull. Assoc. Eng. Geol. 29 (1), 49-60.

Bense, V.F., Gleeson, Loveless, S.E., Bour, O., Scibek, L., 2013. Fault zone hydrogeology. Earth Sci. Rev. 127, 171-192.

Berkowitz, B., 2002. Characterizing flow and transport in fractured geological media: A review. Adv. Water Resour. 25 (8), 861-884.

Billi, A., 2005. Attributes and influence on fluid flow of fractures in foreland carbonates of southern Italy. J. Struct. Geol. 27 (9), 1630-1643.

Binley, A., Winship, P., West, L.J., Pokar, M., Middleton, R., 2002. Seasonal variation of moisture content in unsaturated sandstone inferred from borehole radar and resistivity profiles. J. Hydrol. 267 (3), 160-172.

Black, J.H., Brightman, M.A., 1996. Conceptual model of the hydrogeology of Sellafield. Quart. J. Eng. Geol. Hydrogeol. 29 (1), 83-93.

Bloomfield, J.P., Gooddy, D., Bright, M., Williams, P., 2001. Pore-throat size distributions in Permo-Triassic sandstones from the United Kingdom and some implications for contaminant hydrogeology. Hydrogeol J. 9 (3), 219-230.

Bloomfield, J.P., Moreau, M.F., Newell, A.J., 2006. Characterization of permeability distribution in six lithofacies from the Helsby and Wilmslow sandstone formations of the Cheshire Basin, UK. In: Barker, R.D., Tellam, J.H. (Eds.), Fluid Flow and Solute Movement in Sandstones: The Onshore UK Permo-Triassic Red Bed Sequence. Geol. Soc. London, Spec. Publ. 263, pp. 83-101.

Bottrell, S., Tellam, J.H., Bartlett, R., Hughes, A., 2008. Isotopic composition of sulfate as a tracer of natural and anthropogenic influences on groundwater geochemistry in an urban sandstone aquifer, Birmingham, UK. Appl. Geochem. 23 (8), 2382-2394.

Bouch, J.E., Hough, E., Kemp, S.J., McKervey, J.A., Williams, G.M., Greswell, R.B., 2006. Sedimentary and diagenetic environments of the Wildmoor Sandstone Formation (United Kingdom): implications for groundwater and contaminant transport, and sand production. In: Barker, Tellam (Eds.), Fluid Flow and Solute Movement in Sandstones: The Onshore UK Permo-Triassic Red Bed Sequence. Geol. Soc., London, Spec. Publ., 263, pp. 129-158.

Bradbury, K.R., Borchardt, M.A., Gotkowitz, M., Spencer, S.K., Zhu, J., Hunt, R.J., 2013. Source and transport of human enteric viruses in deep municipal water supply wells. Environ. Sci. Technol. 47 (9), 4096-4103.

Brassington, F. C., 1992. Measurements of head variations within observation boreholes and their implications for groundwater monitoring. Water Environ. J. 6 (3), 91-100.

Brassington, F.C., Walthall, S., 1985. Field techniques using borehole packers in hydrogeological investigation. Quart. J. Eng. Geol. Hydrogeol. 18, 181-193.

British Geological Survey, 2015. Onshore GeoIndex. Geological Map of Great Britain 1:650.000 scale. BGS, Nottingham, England (UK).

Brookfield, M.E., 2004. The enigma of fine-grained alluvial basin fills: the Permo-Triassic (Cumbrian Coastal and Sherwood Sandstone Groups) of the Solway Basin, NW England and SW Scotland. Int. J. Earth Sci. 93 (2), 282-296.

Brookfield, M.E., 2008. Palaeoenvironments and palaeotectonics of the arid to hyperarid intracontinental latest Permian-late Triassic Solway basin (UK). Sediment. Geol. 210 (1), 27-47.

Butler, J.J., 1990. The role of pumping tests in site characterization: Some theoretical considerations. Ground Water 28 (3), 394-402.

Caine, J.S., Evans, J.P., Forster, C.B., 1996. Fault zone architecture and permeability structure. Geology, 24 (11), 1025-1028.

Carminati, E., Cuffaro, M., Doglioni, C., 2009. Cenozoic uplift of Europe. Tectonics 28, (4), doi: 10.1029/2009TC002472.

Cassidy, R., Comte, J. C., Nitsche, J., Wilson, C., Flynn, R., Ofterdinger, U., 2014. Combining multi-scale geophysical techniques for robust hydro-structural characterisation in catchments underlain by hard rock in post-glacial regions. J. Hydrol. 517, 715-731.

Chadwick, R.A., Kirby, G.A., Baily, H.E., 1994. The post-Triassic structural evolution of north-west England and adjacent parts of the East Irish Sea. Proceed, York. Geol. Soc. 50 (1), 91-102.

Chadwick, R.A., 1997. Fault analysis of the Cheshire Basin, NW England. In: Meadows, N.S., Trueblood, S.P., Hardman, M., Cowan, G. (Eds.), Petroleum Geology of the Irish Sea and Adjacent Areas. Geol. Soc. London, Spec. Publ. 124, pp. 297-313.

Chen, Y., Durlofsky, L.J., Gerritsen, M., Wen, X.H., 2003. A coupled local–global upscaling approach for simulating flow in highly heterogeneous formations. Advan. Water Resour. 26 (10), 1041-1060.

Cilona, A., Aydin, A., Johnson, N.M., 2015. Permeability of a fault zone crosscutting a sequence of sandstones and shales and its influence on hydraulic head distribution in the Chatsworth Formation, California, USA. Hydrogeol. J. 23 (2), 405-419.

Clark, L., 1977. The analysis and planning of step drawdown tests. Quart. J. Eng. Geol. Hydrogeol. 10 (2), 125-143.

Colombera, L., Mountney, N.P., McCaffrey, W.D., 2013. A quantitative approach to fluvial facies models: methods and example results. Sedimentology 60 (6), 1526-1558.

Conrad, S.H., Glass, R.J., Peplinski, W.J., 2002. Bench-scale visualization of DNAPL remediation processes in analog heterogeneous aquifers: surfactant floods and in situ oxidation using permanganate. J. Contam. Hydrol. 58 (1), 13-49.

Crook, J.M., Howell, F.T., 1977. Some Field Permeation Properties of Fractured Permian and Triassic Sandstones in Northwest England. J. Press. Vessel Technol. 99 (1), 187-191.

Davison, C.C., Kozak, E.T., 1988. Hydrogeological characteristics of major fracture zones in a granite batholith of the Canadian shield. Canadian/American Conference on Hydrogeology 4. National Water Well Association, pp. 52–59.

Daw, G.P., Howell, F.T., Woodhead, G.A., 1974. The effect of applied stress upon the permeability of some Permian and Triassic sandstones of Northern England. Int. J. Rock Mech. Mining Sci. Abstr. 13 (2), 537-542.

Day-Lewis, F.D., Johnson, C.D., Paillet, F.L., Halford, K.J., 2011. A computer program for flow-log analysis of single holes (FLASH). Ground Water 49 (6), 926-931.

Dewandel, B., Lachassagne, P., Zaidi, F.K. Chandra, S., 2011. A conceptual hydrodynamic model of a geological discontinuity in hard rock aquifers: Example of a quartz reef in granitic terrain in South India. J. Hydrol. 405 (3), 474-487.

Duperret, A., Vandycke, S., Mortimore, R.N., Genter, A., 2012. How plate tectonics is recorded in chalk deposits along the eastern English Channel in Normandy (France) and Sussex (UK). Tectonophysics 581, 163-181.

Eden, R.N., Hazel, C.P., 1973. Computer and graphical analysis of variable discharge pumping tests of wells. Civil Engineering Transactions, Institution of Engineers, Sydney, Australia.

Faulkner, J., Hu, B.X., Kish, S., Hua, F., 2009. Laboratory analog and numerical study of groundwater flow and solute transport in a karst aquifer with conduit and matrix domains. J. Contam. Hydrol. 110 (1), 34-44.

Fienen, M.N., Kitanidis, P.K, Watson, D., Jardine, P., 2004. An application of inverse methods to vertical deconvolution of hydraulic conductivity in a heterogeneous aquifer at Oak Ridge National Laboratory. Mathem. Geol. 36 (1), 101-126.

Fowles, J., Burley, S., 1994. Textural and permeability characteristics of faulted high porosity sandstones. Mar. Petrol. Geol. 11 (5), 608-623

Gellasch, C.A., Bradbury, K.R., Hart D.J., Bahr J.M., 2013. Characterization of fracture connectivity in a siliciclastic bedrock aquifer near a public supply well (Wisconsin, USA). Hydrogeol. J. 21 (2), 383-399.

Gillespie, P.A., Walsh, J.J., Watterson, J., Bonson, C.G., Manzocchi, T., 2001. Scaling relationships of joint and vein arrays from The Burren, Co. Clare, Ireland. J. Struct. Geol. 23 (2), 183-201.

Gooddy**,** D.C., Bloomfield, J.P., Harrold, G., Leharne, S.A., 2002. Towards a better understanding of tetrachloroethene entry pressure in the matrix of Permo-Triassic sandstones. J. Contam. Hydrol. 59 (3), 247-265.

Grass, A.J., 1971. Structural features of turbulent flow over smooth and rough boundaries. J. Fluid Mechan. 50 (2), 233-255.

Griffiths, J., Faulkener, D.R., Alexander, P.E., Worden, R.H, 2016. Deformation band development as a function of intrinsic host-rock properties in Triassic Sherwood Sandstone. In: Armitage, P.J., Butcher, A.R., Churchill, J.M., Csoma, A.E., Hollis, C., Lander, R.H., Omma, J.E., Worden, R.H., (Eds.), Reservoir Quality of Clastic and Carbonate Rocks: Analysis, Modelling, Prediction. Geol. Soc. London Spec. Publ. 435, doi: 10.1144/SP435.11

Gutmanis, J.C., G.W., Lanyon, T.J., Wynn, Watson, C.R., 1998. Fluid flow in faults: a study of fault hydrogeology in Triassic sandstone and Ordovician volcaniclastic rocks at Sellafield, north-west England. Proceed. York. Geol. Soc. 52 (2), 159-175.

Hammond, P.A., 2016. The relationship between methane migration and shale-gas well operations near Dimock, Pennsylvania, USA. Hydrogeol. J. 24 (2), 503-519.

Hartmann, S., Odling, N.E., West, L.J., 2007. A multi-directional tracer test in the fractured Chalk aquifer of E. Yorkshire, UK. J. Contam. Hydrol. 94 (3), 315-331.

Hawkins, A.B., McConnell, B.J., 1992. Sensitivity of sandstone strength and deformability to changes in moisture content. Quart. J. Eng. Geol. Hydrogeol. 25 (2), 115-130.

Hillis, R.R., Holford, S.P., Green, P.F, Doré, A.G., Gatliff, R.W., Stoker, M.S., Thomson, K., Turner, J. P., Underhill, J.R., Williams G. A., 2008. Cenozoic exhumation of the southern British Isles. Geology 36 (5), 371-374.

Hitchmough**,** A.M., Riley, M.S., Herbert, A.W., Tellam, J.H., 2007. Estimating the hydraulic properties of the fracture network in a sandstone aquifer. J. Contam. Hydrol. 93 (1), 38-57.

Holliday, H.D., Jones, N.S., McMillan, A.A., 2008. Lithostratigraphical subdivision of the Sherwood Sandstone Group (Triassic) of the northeastern part of the Carlisle Basin, Cumbria and Dumfries and Galloway, UK. Scottish J. Geol. 44 (2), 97-110.

Howard, K.W.F., 1988. Beneficial aspects of sea–water intrusion. Ground Water 25 (4), 398-406.

Hurst, A., 2000. Natural gamma-ray spectrometry in hydrocarbon-bearing sandstones from the Norwegian Continental Shelf. In: Hurst A., Lovell M.A., Morton A.C. (Eds.), Geological Application of Wireline Logs. Geol. Soc. London Spec. Publ. 48 (1), pp. 211-222.

Huyakorn**,** P.S., Panday, S., Wu, Y.S., 1994. A three-dimensional multiphase flow model for assesing NAPL contamination in porous and fractured media, 1. Formulation. J. Contam. Hydrol. 16 (2), 109-130.

Ixer, R.A., Turner, P., Waugh, B., 1979. Authigenic iron and titanium oxides in Triassic red beds (St. Bees Sandstone), Cumbria, northern England. Geol. J. 14 (2), 179-192.

Lasdon, L.S., Smith., S., 1992. Solving large sparse nonlinear programs using GRG. Orsa J. Comput. 4 (1), 2-15.

Jackson, M.D., Ann H.M., Shuji, Y., Howard, D.J., 2003. Upscaling permeability measurements within complex heterolithic tidal sandstones. Mathemat. Geology 35 (5), 499-520.

Jiang, X.W., Wan, L., Wang, X.S, Hu, B.X., 2009. Estimation of fracture normal stiffness using a transmissivity-depth correlation. Int. J. Rock. Mech. Min. Sci. 46 (1), 51-58.

Jiang, X.W., Wang, X.S., Wan, L. 2010. Semi-empirical equations for the systematic decrease in permeability with depth in porous and fractured media. Hydrogeol. J. 18 (4), 839-850.

Jones, F.O., 1975. A laboratory study of the effects of confining pressure on fracture flow and storage capacity in carbonate rocks. J. Petrol. Technol. 27 (1), 21-27.

Jones, N.S., Ambrose, K., 1994. Triassic sandy braidplain and aeolian sedimentation in the Sherwood Sandstone Group of the Sellafield area, west Cumbria. Proceed. York. Geol. Soc. 50 (1), 61-76.

Kana, A. A., West, L. J., Clark, R.A., 2013. Fracture aperture and fill characterization in a limestone quarry using GPR thin-layer AVA analysis. Near Surf. Geophys. 11 (3), 293-305.

Knott, S.D., 1994. Fault zone thickness versus displacement in the Permo-Triassic sandstones of NW England. J. Geol. Soc. 151 (1), 17-25.

Knott, S.D., Beach, A., Brockbank, P.J., Brown, J.L., McCallum, J.E., Welbon, A.I., 1996. Spatial and mechanical controls on normal fault populations. J. Struct. Geol. 18 (2), 359-372.

Korneva, I., Tondi, E., Agosta, F., Rustichelli, A., Spina, V., Bitonte, R., Di Cuia, R., 2014. Structural properties of fractured and faulted Cretaceous platform carbonates, Murge Plateau (southern Italy). Mar. Petrol. Geol. 57, 312-326.

Lawrence, A., Stuart, M., Cheney, C., Jones, N., Moss, R., 2006. Investigating the scale of structural controls on chlorinated hydrocarbon distributions in the fractured-porous unsaturated zone of a sandstone aquifer in the UK. Hydrogeol. J. 14 (8), 1470-1482.

Le Borgne, T., Bour, O., De Dreuzy, J.R., Davy, P. Touchard, F., 2004. Equivalent mean flow models for fractured aquifers: Insights from a pumping tests scaling interpretation. Water Resour. Res. 40 (3), doi: 10.1029/2003WR002436.

Le Borgne, T., Bour, O., Paillet, F.L., Caudal, J.P., 2006a. Assessment of preferential flow path connectivity and hydraulic properties at single-borehole and cross-borehole scales in a fractured aquifer. J. Hydrol. 328 (1), 347-359.

Le Borgne, T., Paillet, F., Bour, O., Caudal, J.P., 2006b. Cross-Borehole Flowmeter Tests for Transient Heads in Heterogeneous Aquifers. Ground Water 44, (3) 444-452.

Lo, H.C., Chen, P.J., Chou, P.Y., Hsu, S.M., 2014. The combined use of heat-pulse flowmeter logging and packer testing for transmissive fracture recognition. J. Appl. Geophys. 105, 248-258.

Martin, C.D., Davison, C.C., Kozak, E.T., 1990. Characterizing normal stiffness and hydraulic conductivity of a major shear zone in granite, Rock Joints. Balkeema, Rotterdam, Netherlands.

Mathias, S.A., Adrian P.B., Hongbin, Z., 2008. Approximate solutions for Forchheimer flow to a well. J. Hydraul. Engineer. 134 (9), 1318-1325.

Mathias, S.A., Lindsay C.T., 2010. Step-drawdown tests and the Forchheimer equation. Water Resour. Res. 46 (7), doi:10.1029/2009WR008635

McMillan, A.A., Heathcote, J.A., Klinck, B.A., Shepley, M.G., Jackson, C.P., Degnan, P.J., 2000. Hydrogeological characterization of the onshore Quaternary sediments at Sellafield using the concept of domains. Quart. J. Engin. Geol. Hydrogeol. 33 (4), 301-323.

Medici, G., Boulesteix, K., Mountney, N.P., West, L.J., Odling, N.E., 2015. Palaeoenvironment of braided fluvial systems in different tectonic realms of the Triassic Sherwood Sandstone Group, UK. Sediment. Geol. 329, 188-210.

Miall, D., 1977. A review of the braided-river depositional model environment. Earth Sci. Rev. 13 (1), 1-62.

Miall, A.D., 2006. The geology of fluvial deposits. Sedimentary Facies, Basin Analysis and Petroleum Geology. Springer, Berlin, Germany.

Michie, U., 1996. The geological framework of the Sellafield area and its relationship to hydrogeology. Quart. J. Eng. Geol. Hydrogeol. 29 (1), 13-27.

Milodowski, A.E., Gillespie, M.R., Naden, J., Fortey, N.J., Shepherd, T.J., Pearce, J. M., Metcalfe, R., 1998. The petrology and paragenesis of fracture mineralization in the Sellafield area, west Cumbria. Proceed. York. Geol. Soc. 52 (2), 215-241.

Mobile, M., Widdowson, M., Stewart, L., Nyman, J., Deeb, R., Kavanaugh, M., Mercer, J., Gallagher, D., 2016. In-situ determination of field-scale NAPL mass transfer coefficients: Performance, simulation and analysis. J. Contam. Hydrol. 187, 31-46.

Mohamed, E.A., Worden, R.H., 2006. Groundwater compartmentalisation: a water table height and geochemical analysis of the structural controls on the subdivision of a major aquifer, the Sherwood Sandstone, Merseyside, UK. Hydrol. Earth System Sci. Discuss. 10 (1), 49-64.

Molz, F.J., Morin, R.H., Hess, A.E., Melville, J.G., Guven, O., 1989. The impeller meter for measuring aquifer permeability variations: Evaluation and comparison with other tests. Water Resour. Res. 25 (7), 1677-1683.

Moore, C.C., 1902. The study of the volume composition of rocks, and its importance to the geologist. Proceed. Liverpool Geol. Soc., 9, 129-162.

Morin, R.H., Carleton, G.B., Poirier, S., 1997. Fractured-aquifer hydrogeology from geophysical logs, the Passaic Formation, New Jersey. Ground Water 35 (2), 328-338.

Morton, G.H., 1870. Anniversary address by the President. Proceed. Liverpool Geol.

Soc., Session Twelfth, 1-29.

Mountney, N.P., Thompson, D.B., 2002. Stratigraphic evolution and preservation of aeolian dune and damp/wet interdune strata: an example from the Triassic Helsby Sandstone Formation, Cheshire Basin, UK. Sedimentology 49 (4), 805-833.

Neuman, S.P., Di Federico, V., 2003. Multifaceted nature of hydrogeologic scaling and its interpretation. Rev. Geophys. 41 (3), doi: 10.1029/2003RG000130.

Newell, A.J., Shariatipour, S.M., 2016. Linking outcrop analogue with flow simulation to reduce uncertainty in sub-surface carbon capture and storage: an example from the Sherwood Sandstone Group of the Wessex Basin, UK. In: M. Bowman, H.R.

Smyth, T.R. Good, S.R. Passey, J.P.P. Hirst, Jordan, C.J., (Eds.), The Value of Outcrop Studies in Reducing Subsurface Uncertainty and Risk in Hydrocarbon Exploration and Production. Geol. Soc. London, Spec. Publ. 436, doi:10.1144/SP436.2.

Nirex, 1992a. Liquid Permeability - Gas Permeability Correlation for Permo-Trias Samples from Sellafield Boreholes Nos 2 3 5 and 7. Nirex Ltd Report 226. BGS, Nottingham (UK).

Nirex, 1992b. The Geology and Hydrogeology of Sellafield. NIREX Ltd Report 263. BGS, Nottingham (UK).

Nirex, 1992c. Permeability and Porosity results for samples from the Permo-Trias Carboniferous and Borrowdale Volcanic Group of Sellafield Borehole 10. Nirex Ltd Report 226. BGS, Nottingham (UK).

Nirex, 1993a. The Geology and Hydrogeology of the Sellafield Area: Interim Assessment. Nirex Ltd Report 524. BGS, Nottingham, England (UK).

Nirex, 1993b. Permeability and Porosity Results for samples from The Permo-Trias and Borrowdale Volcanic Group of Sellafield Borehole RCF3 and the Permo-Trias of Sellafield Borehole RCM2 Nirex Ltd Report 806. BGS, Nottingham, England (UK).

Nirex, 1993c. Permeability and porosity results for samples from the Permo-Triassic and Carboniferous of Sellafield Boreholes 13A 13B 14A RCF1 and RCF2. Nirex Ltd Report 818. BGS, Nottingham, England (UK).

Nirex, 1997. Sellafield Geological and Hydrogeological Investigations. Sedimentology and sedimentary architecture of the St Bees Sandstone Formation in West Cumbria. Report SA/97/023. BGS, Nottingham, England (UK).

Noushabadi, M,R., Jourde, J.H., Massonnat, G., 2011. Influence of the observation scale on permeability estimation at local and regional scales through well tests in a fractured and karstic aquifer (Lez aquifer, Southern France). J. Hydrol. 403 (3), 321-336.

Odling, N.E., Gillespie, P., Bourgine, B., Castaing, C., Chiles, J.P., Christensen, N.P., Fillion, E., Genter, A., Olsen, C., Thrane, Trice, R., 1999. Variations in fracture system geometry and their implications for fluid flow in fractured hydrocarbon reservoirs. Petrol. Geosci. 5 (4), 373-384.

Odling, N.E., Roden, J.E., 1997. Contaminant transport in fractured rocks with significant matrix permeability, using natural fracture geometries. J. Contam. Hydrol. 27 (3), 263-283.

Odling, NE, West, LJ, Hartmann S, Kilpatrick, A., 2013. Fractional flow in fractured chalk; a flow and tracer test revisited. J. Contam. Hydrol. 147, 96-111.

Odonne, F., Lézin, C., Massonnat, G., Escadeillas, G., 2007. The relationship between joint aperture, spacing distribution, vertical dimension and carbonate stratification: An example from the Kimmeridgian limestones of Pointe-du-Chay (France). J. Struct. Geol. 29 (5), 746-758.

Oostrom, M., Hofstee, C., Walker, R.C., J.H., Dane, J.H., 1999. Movement and remediation of trichloroethylene in a saturated heterogeneous porous medium: 1. Spill behavior and initial dissolution. J. Contam. Hydrol. 37 (1), 159-178.

Paillet, F.L., 1998. Flow modeling and permeability estimation using borehole flow logs in heterogeneous fractured formations. Water Resour. Res. 34 (5), 997-1010

Paillet, F.L., 2000. A field technique for estimating aquifer parameters using flow log data. Ground Water 38 (4), 510-521.

Paillet, F.L., 2004. Borehole flowmeter applications in irregular and large-diameter boreholes. J. Appl. Geophys. 55, (1), 39-59.

Parker, A.H., L. West, J.L., Odling, N.E., Bown, T.R., 2010. A forward modeling approach for interpreting impeller flow logs. Ground Water 48 (1), 79-91.

Pittman, E.D., 1981. Effect of fault-related granulation on porosity and permeability of quartz sandstones, Simpson Group (Ordovician), Oklahoma. AAPG Bullet. 65 (11), 2381-2387.

Pokar, M., West, L.J., Odling, N.E., 2006. Petrophysical characterization of the Sherwood Sandstone from East Yorkshire, UK. In: Barker, R.D., Tellam, J.H. (Eds.), Fluid Flow and Solute Movement in Sandstones: The Offshore UK Permo-Triassic Red Bed Sequence. Geol. Soc. London, Spec. Publ. 263, pp. 103-118.

Powell, K.L., Taylor, R.G., Cronin, A.A., Barrett, M.H., Pedley, S., Sellwood, J., Trowsdale, S.A., Lerner, D.N., 2003. Microbial contamination of two urban sandstone aquifers in the UK. Water Resour. 37 (2), 339-352.

Price, M., Morris, B., Robertson, A., 1982. A study of intergranular and fissure permeability in Chalk and Permian aquifers, using double-packer injection testing. J. Hydrol. 54 (4), 401-423.

Qin, R., Wu, Y., Xu, Z., Xie, D., Zhang, C., 2013. Numerical modeling of contaminant transport in a stratified heterogeneous aquifer with dipping anisotropy. Hydrogeol. J. 21 (6), 1235-1246.

Reks, I.J., Gray, D.R., 1982. Pencil structure and strain in weakly deformed mudstone and siltstone. J. Struct. Geol. 4 (2), 161-176.

Rider, M.H., 2000. Gamma-ray log shape used as a facies indicator: critical analysis of an oversimplified methodology. In: Hurst A., Lovell M.A., Morton A.C. (Eds.), Geological Application of Wireline Logs. Geol. Soc., London, Spec. Publ. 48 (1), pp. 27-37.

Rivett, M.O., Lerner, D.N., Lloyd, J.W., Clark, L., 1990. Organic contamination of the Birmingham aquifer, UK. J. Hydrol. 113 (1), 307-323.

Rivett, M.O., Wealthall, G.P., Dearden, R.A., McAlary, T.A., 2011. Review of unsaturated-zone transport and attenuation of volatile organic compound (VOC) plumes leached from shallow source zones. J. Contam. Hydrol. 123 (3), 130-156.

Rivett, M.O., Turner, R.J., Glibbery, P., Cuthbert, M.O., 2012. The legacy of chlorinated solvents in the Birmingham aquifer, UK: Observations spanning three decades and the challenge of future urban groundwater development. J. Contam. Hydrol. 140, 107-123.

Roques, C., Bour, O., Aquilina, L., Dewandel, B., Leray, S., Schroetter, J.M., Longuevergne, L., Le Borgne, T., Hochreutener, R., Labasque, T., Lavenant, N., 2014. Hydrological behavior of a deep sub-vertical fault in crystalline basement and relationships with surrounding reservoirs. J. Hydrol. 509, 42-54.

Runkel, A.C., Tipping, R.G., Alexander, E.C., Alexander, S.C., 2006. Hydrostratigraphic characterization of intergranular and secondary porosity in part of the Cambrian sandstone aquifer system of the cratonic interior of North America: Improving predictability of hydrogeologic properties. Sediment. Geol. 184 (3), 281-304.

Rustichelli, A., Agosta, F., Tondi, E., Spina, V., 2013. Spacing and distribution of bed-perpendicular joints throughout layered, shallow-marine carbonates (Granada Basin, southern Spain). Tectonophysics 582, 188-204.

Rustichelli, A., Di Celma, C., Tondi, E., Bianucci, G., 2016. Deformation within the Pisco basin sedimentary record (southern Peru): Stratabound orthogonal vein sets and their impact on fault development. J. South America Earth Sci. 65, 79-100.

Rutqvist, J., Tsang, C.F., 2003. Analysis of thermal–hydrologic–mechanical behavior near an emplacement drift at Yucca Mountain. J. Contam. Hydrol. 62, 637-652.

Smedley, P.L., Edmunds, W.B., 2002. Redox Patterns and Trace-Element Behavior in the East Midlands Triassic Sandstone Aquifer, UK. Ground Water 40, 44-58.

Sethi, R., 2011. A dual-well step drawdown method for the estimation of linear and non-linear flow parameters and wellbore skin factor in confined aquifer systems. J. Hydrol. 400 (1), 187-194.

Seymour, K.J., Ingram, J.A., Gebbett, S.J., 2006. Structural controls on groundwater flow in the Permo-Triassic sandstones of NW England. In: Barker, R.D., Tellam, J.H. (Eds.), Fluid Flow and Solute Movement in Sandstones: The Onshore UK Permo-Triassic Red Bed Sequence. Geol. Soc. London, Spec. Publ. 263, p.p. 169-185.

Smith, B., 1924. On the West Cumberland Brockram and its associated rocks. Geolog. Magazine 61 (7), 289-308.

Steele, A., Lerner, D.N., 2001. Predictive modelling of NAPL injection tests in variable aperture spatially correlated fractures. J. Contam. Hydrol. 49 (3) 287-310.

Streetly, M., C. Chakrabarty, McLeod, R., 2000. Interpretation of pumping tests in the Sherwood Sandstone Group, Sellafield, Cumbria, UK. Quart. J. Eng. Geol. Hydrogeol. 33 (4), 281-299.

Streetly, M.J., Heathcote, J.A., Denghan, P.J., 2006. Estimation of vertical diffusivity from seasonal fluctuations in groundwater pressures in deep boreholes near Sellafield, NW England. In: Barker, R.D., Tellam, J.H. (Eds.), Fluid Flow and Solute Movement in Sandstones: The Offshore UK Permo-Triassic Red Bed Sequence. Geol. Soc. London, Spec. Publ. 263 (1), pp. 103-118.

Strong, G.E., Milodowski, A.E., Pearce, J.M., Kemp, S.J., Prior, S.V., Morton, A.C., 1994. The petrology and diagenesis of Permo-Triassic rocks of the Sellafield area, Cumbria. Proceed. York. Geol. Soc. 50 (1), 77-89.

Tellam, J.H., 2004. 19th century studies of the hydrogeology of the Permo-Triassic Sandstones of the northern Cheshire Basin, England. In: Mather, J. (Ed.), 200 Years of British Hydrogeology. Geological Society, London, Spec. Publ. 225, p.p. 89-105.

Tellam, J.H., Barker, R.D., 2006. Towards prediction of satured-zone pollutant movement in groundwaters in fractured permeable-matrix aquifers: the case of the UK Permo-Triassic sandstones. In: Barker, R.D., Tellam, J.H. (Eds.), Fluid Flow and Solute Movement in Sandstones: The Onshore UK Permo-Triassic Red Bed Sequence. Geol. Soc. London, Spec. Publ. 263, pp.1-48.

Terzaghi, R.D., 1965. Sources of errors in joint surveys. Geotechnique 15 (3), 287-304

Thiem, G., 1906. Hydrologische Methoden. J.M. Gebhardt, Leipzig, pp. 56

Theis, C.V., 1935. The relation between the lowering of the piezometric surface and the rate and duration of discharge of a well using groundwater storage. Trans. Amer. Geophys. Union 16 (2), 519-524.

Thompson, D.B., 1970. Sedimentation of the Triassic (Scythian) red pebbly sandstones in the Cheshire Basin and its margins. Geol. J. 7, 183-216.

Torabi, A., Fossen, H., 2009. Spatial variation of microstructure and petrophysical properties along deformation bands in reservoir sandstones. AAPG Bullet. 93 (7), 919-938.

Tsang, C.F., Hufschmied, P., Hale, F.V., 1990. Determination of fracture inflow parameters with a borehole fluid conductivity logging method. Water Resour. Res. 26 (4), 561-576.

Tueckmantel, C., Fisher, Q.J., Grattoni, C.A., Aplin, A.C., 2012. Single-and two-phase fluid flow properties of cataclastic fault rocks in porous sandstone. Marine Petrol. Geol. 29 (1), 129-142.

Turner, P., 1981. Relationship between magnetic components and diagenetic features in reddened Triassic alluvium (St Bees Sandstone, Cumbria, UK). Geophys. J. Intern. 67 (2), 395-413.

Van Tonder, G.J., Botha, J.F., Chiang, W-H., Kunstmann, H., Xu, Y., 2001. Estimation of the sustainable yields of boreholes in fractured rock formations. J. Hydrol. 241 (1), 70-90.

Wakefield, O.J, Hough, E., Peatfield, A.W., 2015. Architectural analysis of a Triassic fluvial system: the Sherwood Sandstone of the East Midlands Shelf, UK. Sediment. Geol. 327, 1-13.

Wealthall, G.P., Steele, A., Bloomfield, J.P., Moss, R.H., Lerner, D.N., 2001. Sediment filled fractures in the Permo-Triassic sandstones of the Cheshire Basin: observations and implications for pollutant transport. J. Contam. Hydrol. 50 (1), 41-51.

West, L.J., Truss, S.W. 2006. Borehole time domain reflectometry in layered sandstone: Impact of measurement technique on vadose zone process identification. J. Hydrol. 319 (1), 143-162.

Williams, J.H., Johnson, C.D., 2004. Acoustic and optical borehole-wall imaging for fractured-rock aquifer studies. J. Appl. Geophys. 55 (1), 151-159.

Wray, R.A.L., 1997. A global review of solutional weathering forms on quartz sandstones. Earth Sci. Rev. 42 (3), 137-160.

Yang, Y., Aplin, A.C., 2007. Permeability and petrophysical properties of 30 natural samples. J. Geophys. Res: Solid Earth. 112 (B03), doi: 10.1029/2005JB004243.

Yates, P.G. J., 1992. The material strength of sandstones of the Sherwood Sandstone Group of north Staffordshire with reference to microfabric. Quart. J. Eng. Geol. Hydrogeol. 25 (2), 107-113.

Zhang, H., Hiscock, K.M., 2010. Modelling the impact of forest cover on groundwater resources: A case study of the Sherwood Sandstone aquifer in the East Midlands, UK. J. Hydrol. 392 (3), 136-149.

Zhang, H., Hiscock, K.M., 2011. Modelling the effect of forest cover in mitigating nitrate contamination of groundwater: A case study of the Sherwood Sandstone aquifer in the East Midlands, UK. J. Hydrol. 399 (3), 212-225.

Zheng, S. Y., Corbett, P. W., Ryseth, A., Stewart, G., (2000). Uncertainty in well test and core permeability analysis: a case study in fluvial channel reservoirs, northern North Sea, Norway. AAPG Bullet. 84 (12), 1929-1954.

Zoback, M.D., Byerlee, J.D., 1975. Permeability and effective stress: geologic notes. AAPG Bullet. 59 (1), 154-158.

Zhu, C., Burden, D.S. 2001. Mineralogical compositions of aquifer matrix as necessary initial conditions in reactive contaminant transport models. J. Contam. Hydrol. 51 (3), 145-161.

Table captions

Table 1. Construction details and distance from mapped fault traces for the six logged wells.

Table 2. Vertical spacing data for fracture and sedimentary heterogeneities in the six logged wells.

Table. 3. Fracture spacing and mechanical layer thickness data from scanlines of outcropping rock faces (for key see Fig. 1b).

Table 4. Summary of transmissivity values from all pumping tests data available for the 6 studied wells which also includes flow rates of step tests and transmissivity from the upscaling of K_h geometric mean of cored sandstone plugs.

Table 5. Parameters computed from the FLASH program for Thornhill Trial, Bridge End Trial and Black Ling wells.

Table 6. Parameters computed from flow log analysis for Pallaflat Reservoir and Ellergill Bridge wells using equation (3).

Table 7. Transmissivity ranges for the shallow (this work; Allen et al., 1997) and deep investigations (Streetly et al., 2000) of the St Bees Sandstone aquifer.

Figure captions

Fig. 1 Study area. (a) Map depicting surface expression of the Sherwood Sandstone Group (yellow colour) in England, UK (Redrawn from Wakefield et al., 2015), (b) Geological map of the field site with stratigraphic column and location of the scanlines (SL 1-10) and of the 6 logged wells (Redrawn from British Geological

Survey, 2015): Black Ling (BL), Bridge End Trial (BT), Ellergill Bridge (EB), Pallaflat Reservoir (PR), Rottington Trial (RT), Thornhill Trial (TH).

Fig. 2 St Bees Sandstone Formation. (a) Photograph and panel of St Bees Sandstone Formation in a cliff section at Fleswick Bay. The exposure shows the layered nature of the St Bees Sandstone aquifer with beds 1-1.8 m thick commonly separated by white silty sandstone beds (transparent blue). Joints (yellow) are largely truncated by individual bed parallel discontinuities (white), (b) Extensional fault: '1' principal fault plane highlighted by water seepage, '2' fault related open fractures locally occurring as conjugate sets, '3' bedding-parallel fracture cutting the fault structure, '4' detail of granulation seams.

Fig. 3 Principal heterogeneities in the St Bees Sandstone aquifer and structure picking of discontinuities; (a) white siltstones (black dashed lines), (b) mudstones (black dashed lines) and bedding plane fractures (red solid lines), (c) fault cataclasite with open fractures (red solid lines) and small cavities, (d) White sandstone (black dashed line) and medium angle joints (red solid lines) cutting (Gs) granulation seams (e.g., white sandstone - black dashed lines), (e) bed-parallel fractures enlarged by small cavities, (f) sub-vertical joint partially filled by calcite veins.

Fig. 4 Wireline logs from Rottington Trial well showing the geophysical response of (1) white sandstone and (2) mudstone

Fig. 5 Stereoplots (upper hemisphere, equal area); (a) Pole diagrams of fractures for all wells, (b) Pole diagrams of sedimentary heterogeneities for all wells, (c) Mean vectors of fracture families and sedimentary heterogeneities in wells characterized by SW structural dip; trend, plunge and magnitude of mean vectors are reported in brackets, (d) Mean vectors of fracture families and sedimentary heterogeneities in wells characterized by SE structural dip; trend, plunge and magnitude of mean vectors are reported in brackets.

Fig. 6 Stratabound-type fractures; (a) Stereoplots (upper hemisphere, equal area) which includes rose diagrams, Kamb contours (contouring area = 1.5% of net area) and grouping of joints families (S3, S4, S5, S6) from ten scan line surveys carried out in five different fracturing stations in the St Bees area, (b) Conceptual model of the stratabound fracturing system in the St Bees Sandstone aquifer.

Fig. 7 Pumping test data; (a) Drawdown and recovery vs time curves of step tests for the six pumped wells, (b) Observed and modelled step-test drawdown for Black Ling

and Bridge End Trial wells, (c) Drawdown and recovery vs time curves for the six studied wells when pumped at a constant flow rate.

Fig. 8 Fluid logging in wells far from mapped fault traces; fluid conductivity, temperature and velocity logs and modelled flow rate (FLASH generated) profiles for (a) Thornhill Trial and (b) Bridge End Trial wells.

Fig. 9 Fluid logging in wells in fault zones; logs of fluid conductivity, temperature and velocity and model flow rate (FLASH or equation. (3) generated) profiles for (a) Black Ling. Calliper and flow velocity logs for (b) Pallaflat Reservoir and (c) Ellergill Bridge

Fig. 10 Box plots summarising the statistics of the available pumping tests in the St Bees Sandstone aquifer: shallow ≤ 180 m (box plot A) and deep > 180 m (box plot B).

Fig. 11 Conceptual model of the flow system in a fractured well-lithified fluvial sandstone aquifer. (a) Water flow in a shallow sandstone aquifer in: (1) fault core and internal damage zone, (2) external fault damage zone, (3) area not affected by faulting. (b) Typical sedimentary units and water flow in a deep well lithified fluvial sandstone aquifer dominated by (1) matrix flow in areas far away from fault zones, (2) both matrix and fracture flow in fault cores and damage zones.

Supplementary material captions

Table S1 Summary of transmissivity and parameters (step test flow rate, formation loss, turbulent well loss) used for the Eden and Hazel (1973) analysis.

Table S2 Parameters computed by the FLASH program for the Rottington Trial well.

Fig. S1. Observed and program generated step-test drawdown with indication of residual mean (Rm) and residual standard deviation (Rsd) from for Ellergill Bridge, Pallaflat Reservoir, Rottington Trial and Thornhill Trial wells.

Fig. S2 Fluid logging in the un-faulted area of the Rottington Trial well; flow conductivity, temperature and flow rate (FLASH program) profiles in ambient and pumped conditions.

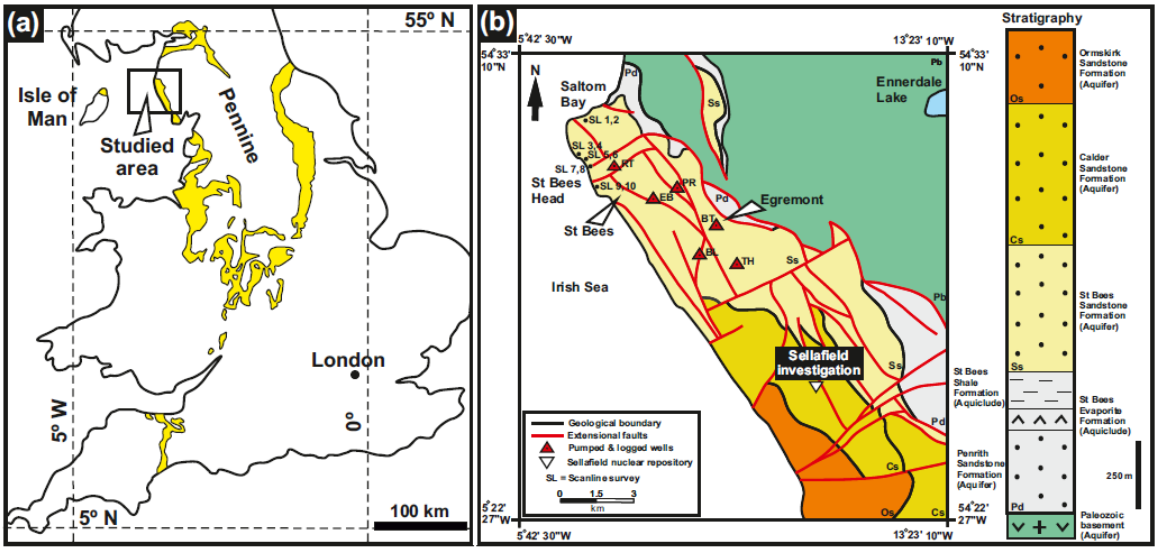

Fig. 1

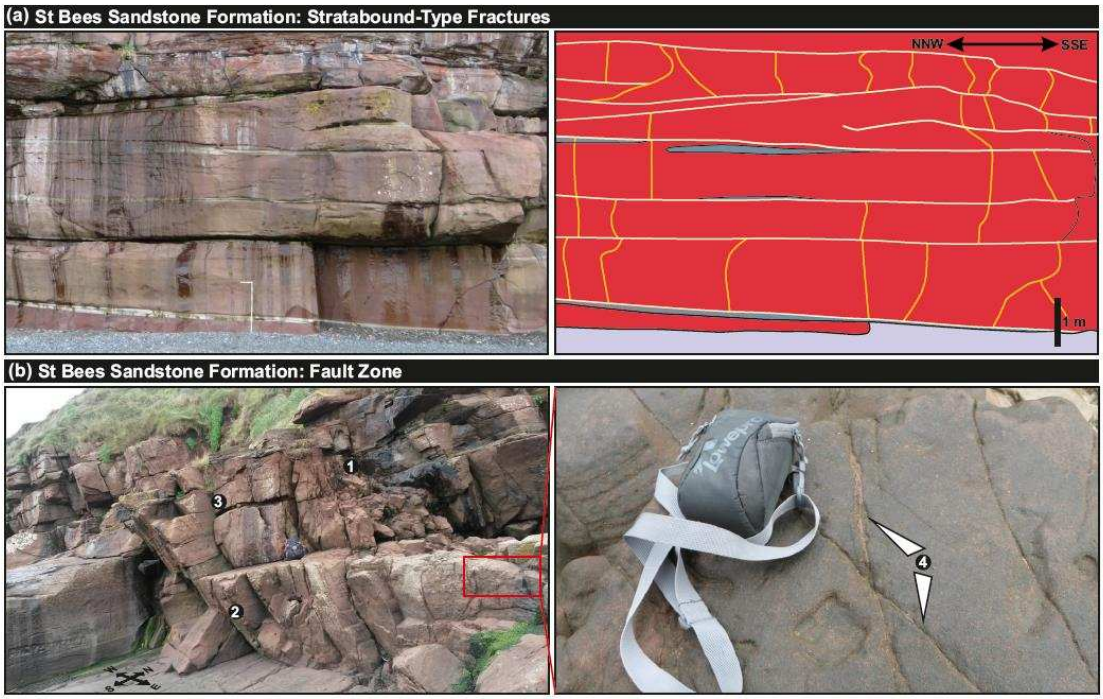

Fig. 2

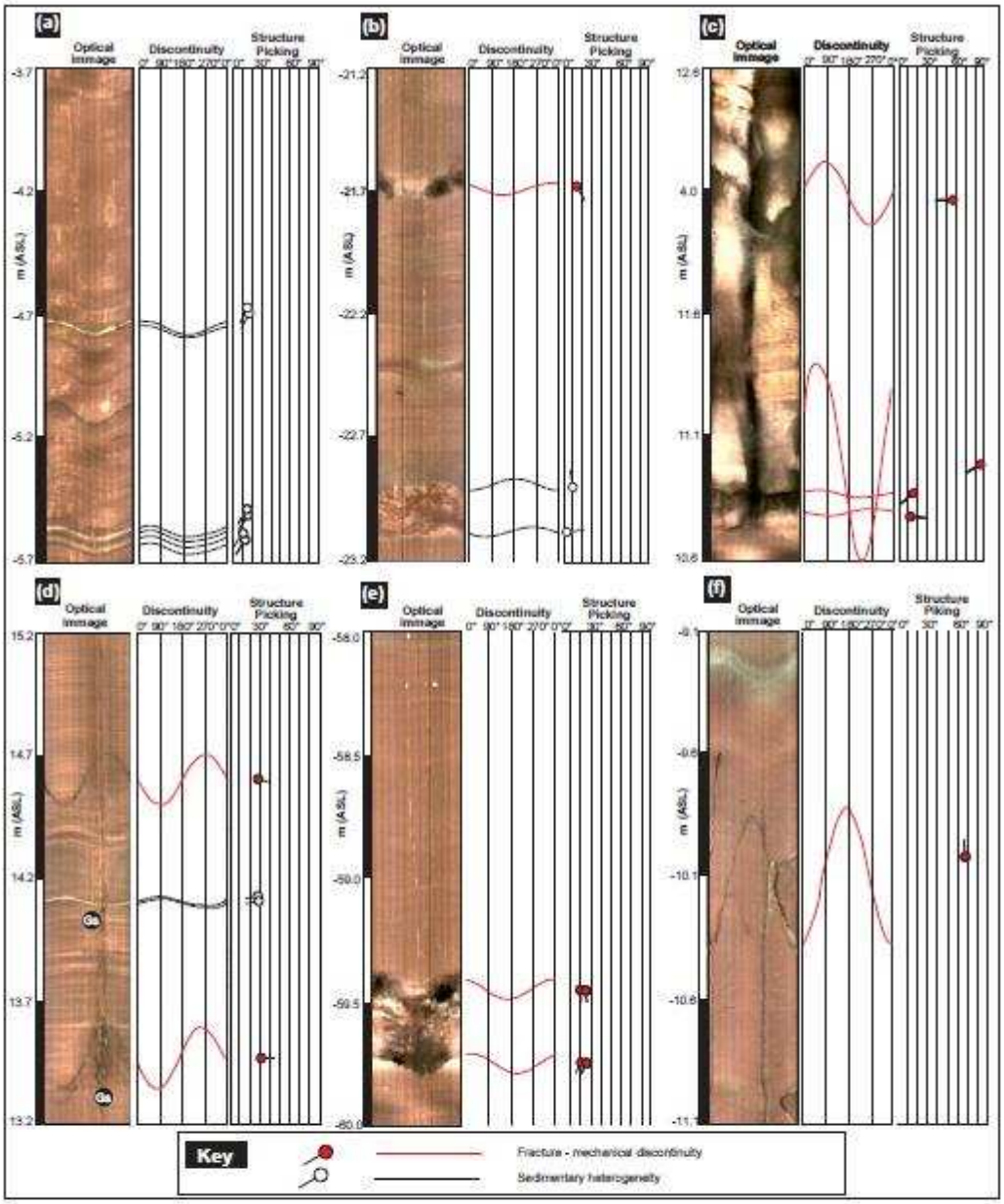

Fig. 3

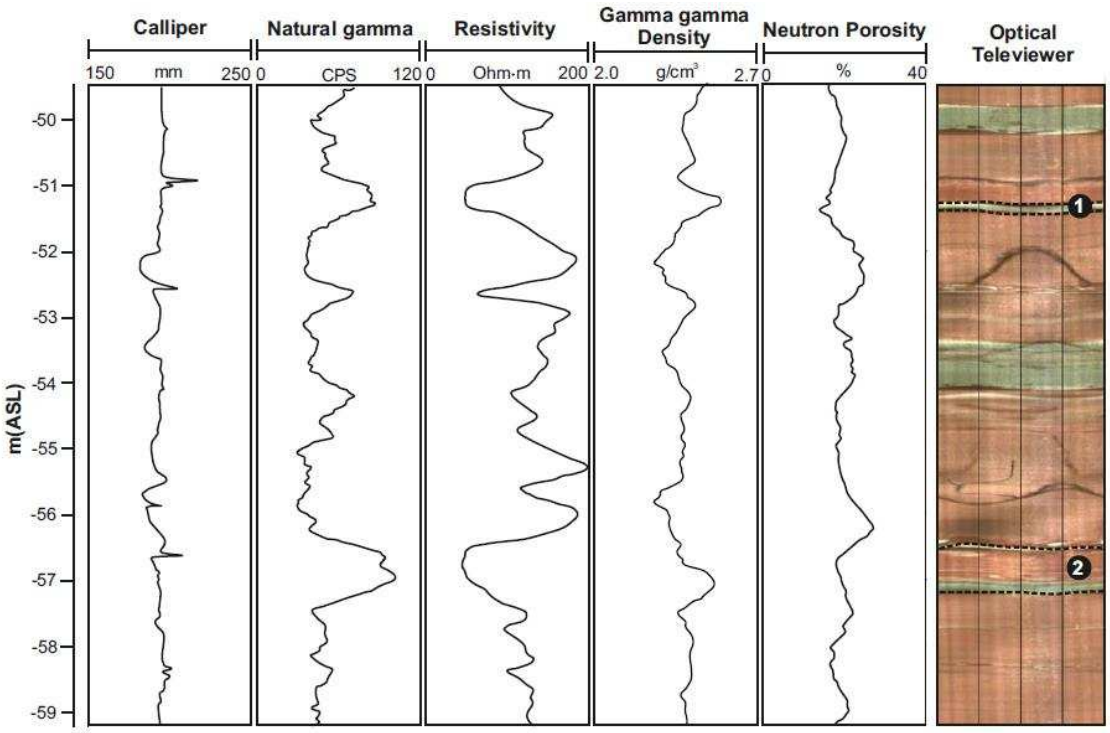

Fig. 4

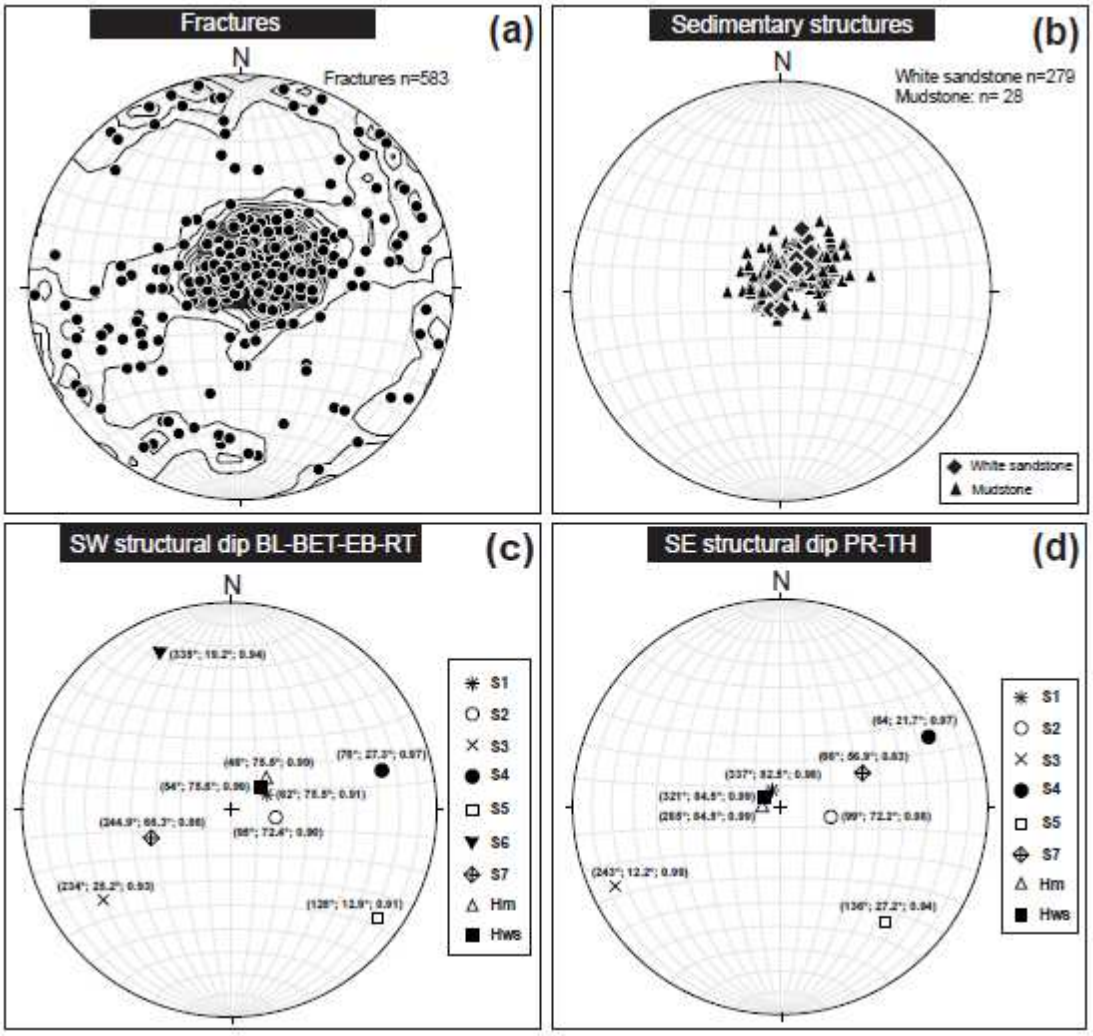

Fig. 5

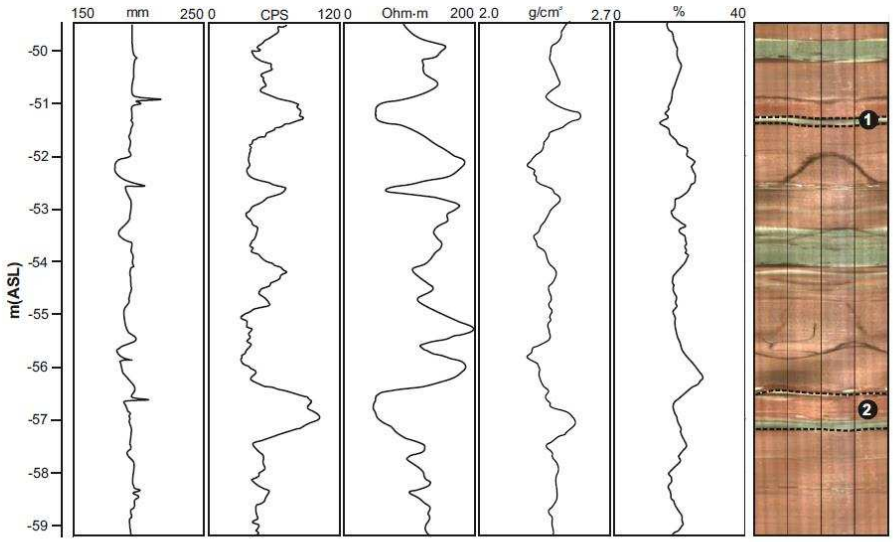

Fig. 6

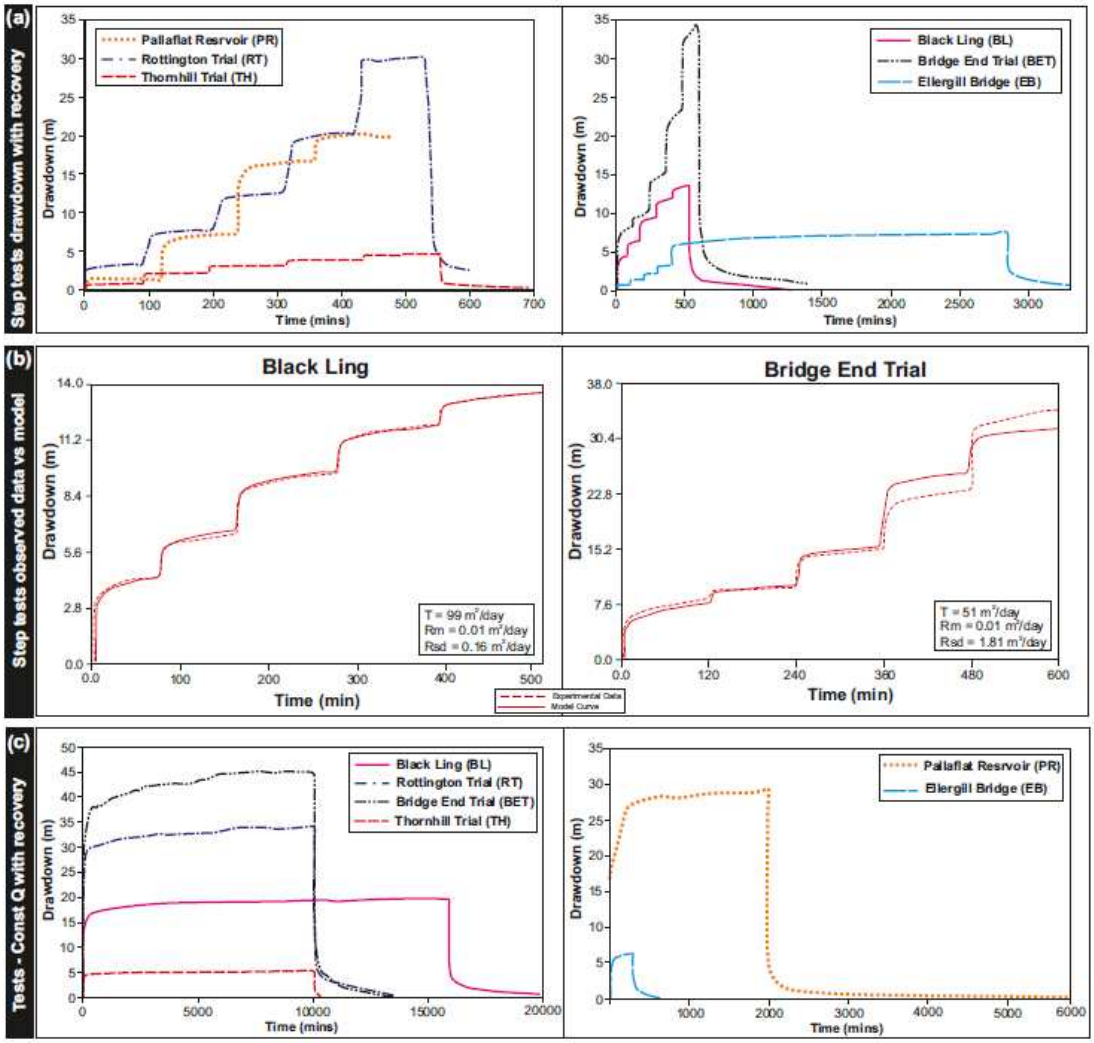

Fig. 7

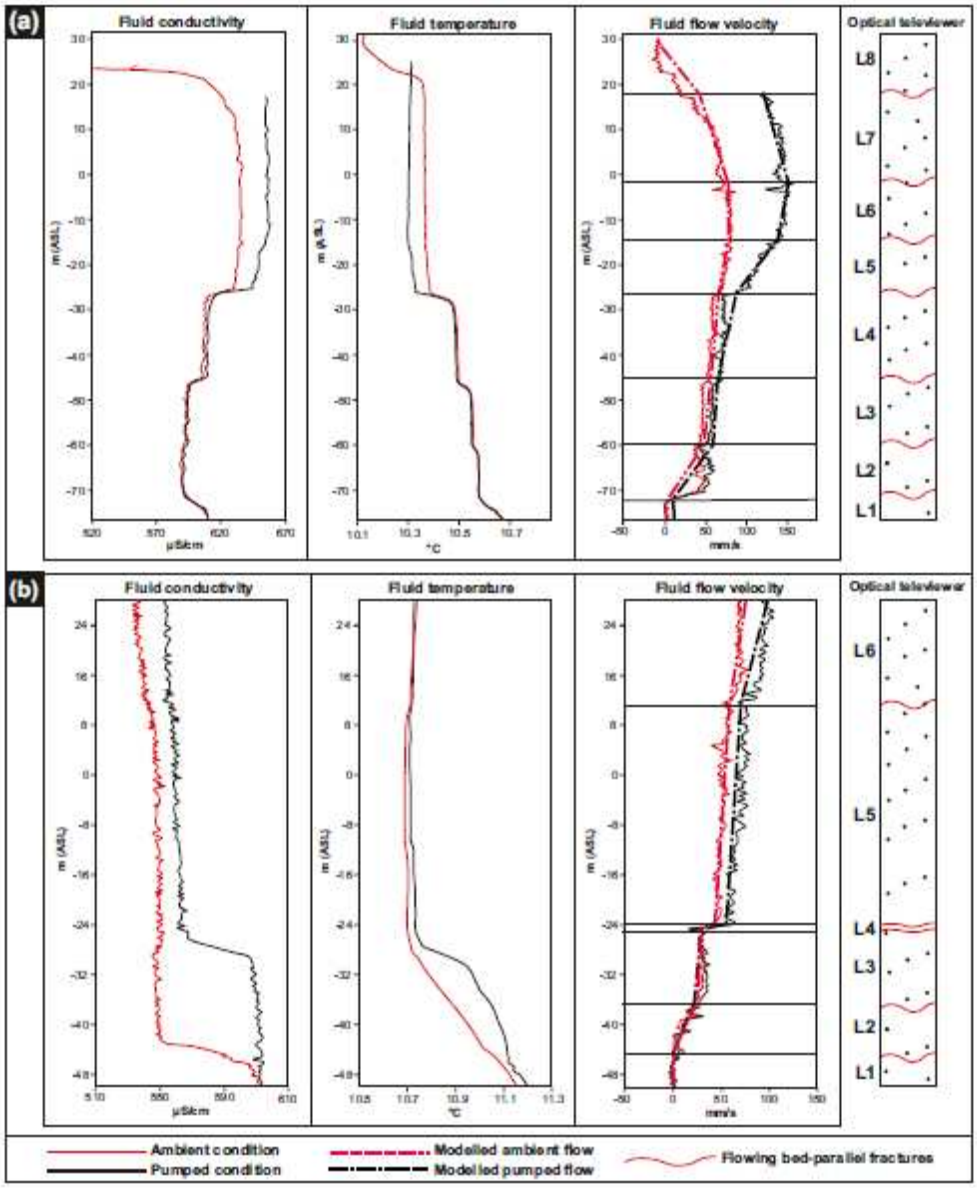
(a)
Fluid conductivity
Fluid temperature
Fluid flow velocity
Optical televiewer
L8
L7
L6
L5
L4
L3
L2
L1
m (ASL)
µS/cm
°C
mm/s
(b)
Fluid conductivity
Fluid temperature
Fluid flow velocity
Optical televiewer
L6
L5
L4
L3
L2
L1
m (ASL)
µS/cm
°C
mm/s
Ambient condition
Pumped condition
Modelled ambient flow
Modelled pumped flow
Flowing bed-parallel fractures

Fig. 8

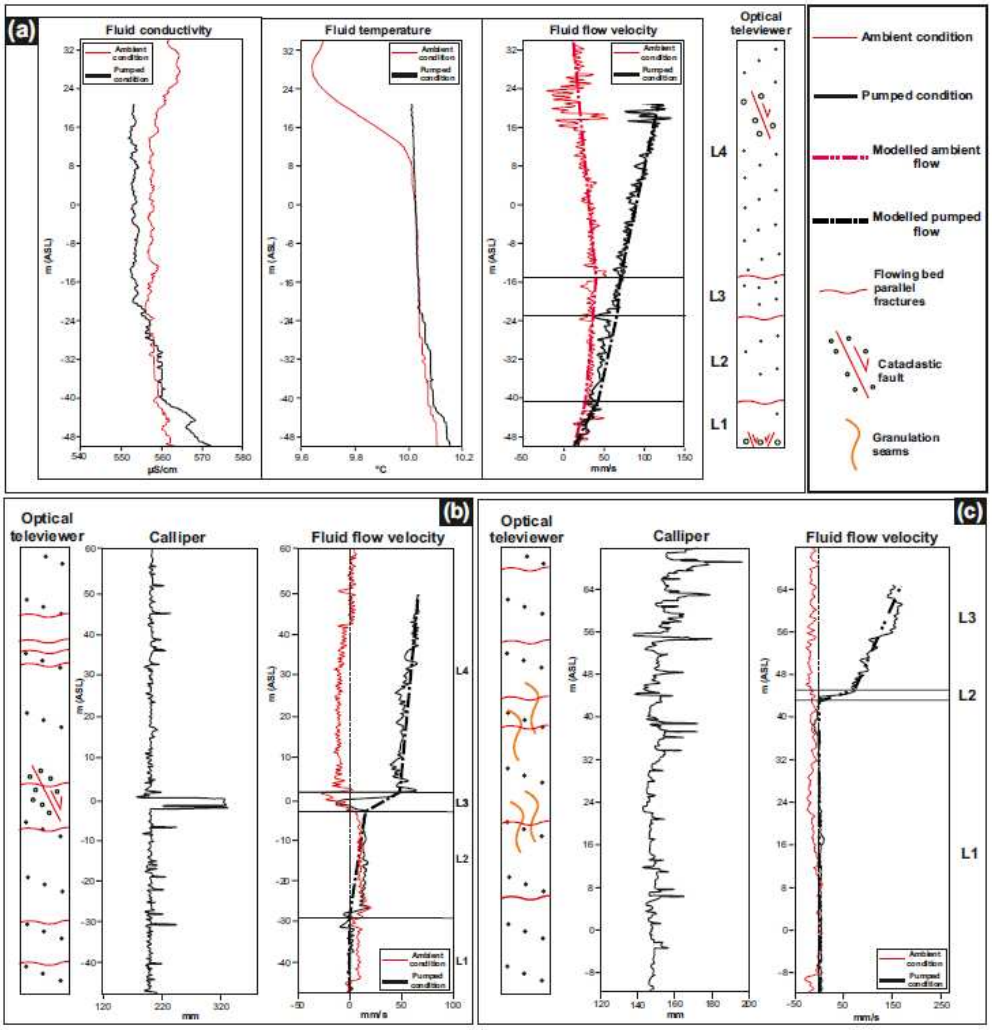

Fig. 9

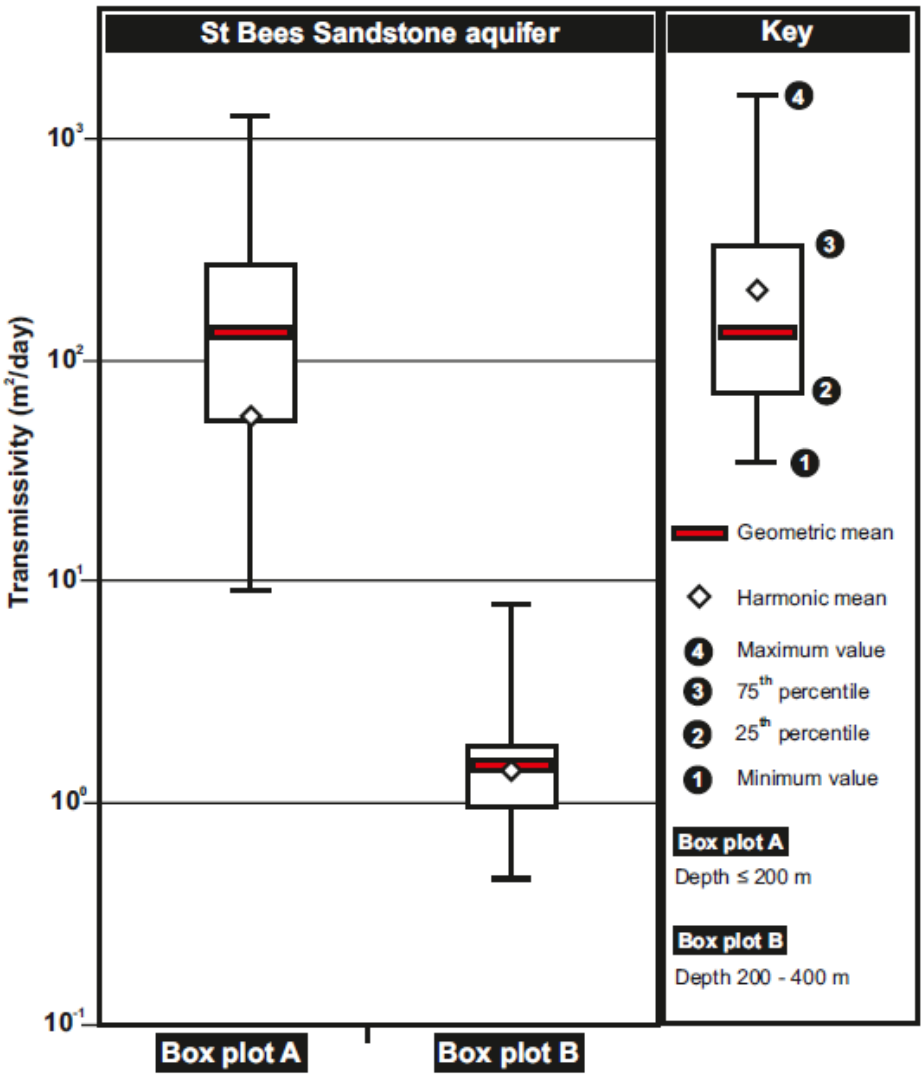

Fig. 10

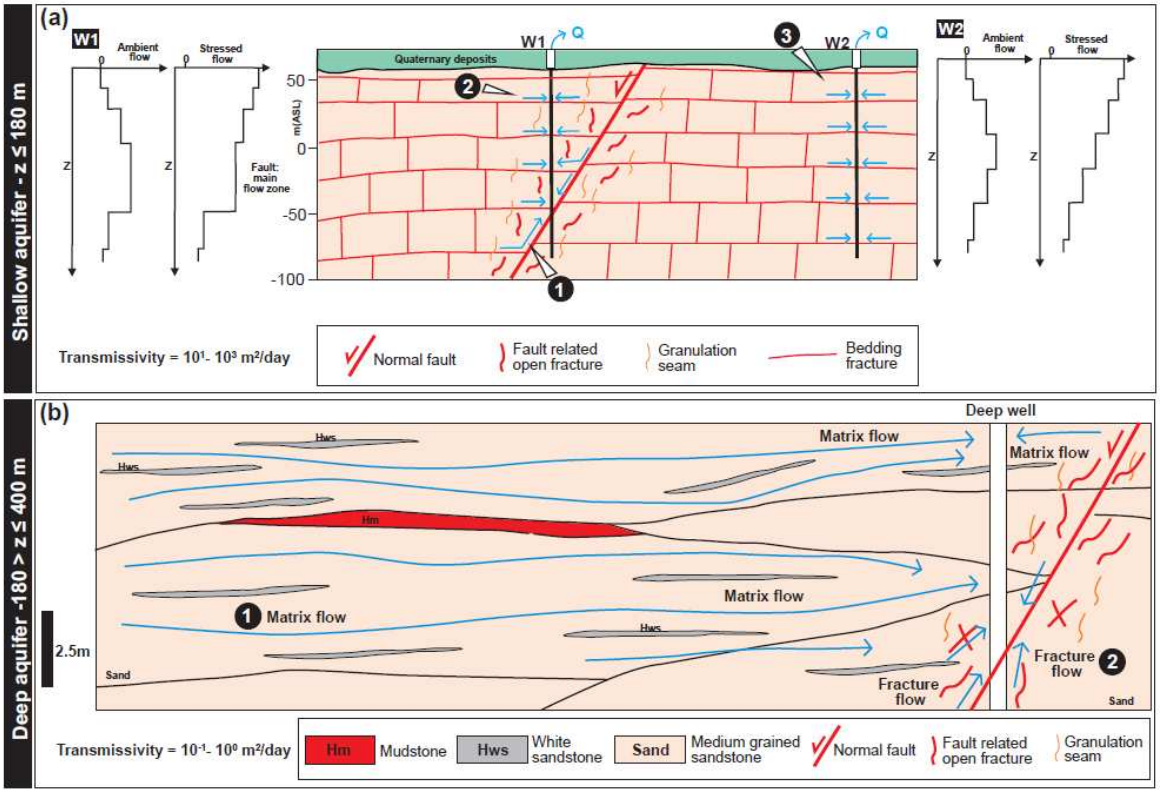

Fig. 11

Field site/well name	Borehole diameter (m)	Casing depth (m) BGL; ASL	Screen length (m)	Distance from mapped fault trace (m)
Black Ling	0.20	26; 34	84	0
Bridge End Trial	0.20	14; 28	76	95
Ellergill Brdge	0.15	21; 72	84	10
Pallaflat Resrevoir	0.20	6; 98	146	0
Rottington Trial	0.20	7; 46	111	55
Thornhill Trial	0.20	10; 31	107.5	340

Table. 1

Type of heterogeneity	Code	Population (n.)	Vertical spacing range (m)	Average vertical spacing (m)	Standard deviation σ (m)
Tectonic-reactivation master beds	S1	439	0.01 - 6.54	1.2	1.27
Tectonic-reactivation cross beds	S2	39	0.05 - 20.01	7.8	7.77
Tectonic-stratabound joints	S3+S4	42	0.48 - 30.16	8.3	7.68
Tectonic-stratabound joints	S5+S6	13	3.54 - 42.06	16.7	12.46
Tectonic/artificial fractures	S7	50	0.05 - 54.56	5.7	7.43
Sedimentary (i) mudstone	Hm	28	0.1 - 50.55	16.1	15.55
Sedimentary (ii) White sandstone	Hws	279	0.02 - 19.35	2.1	2.38

Table 2.

Station; scanline code	Scanline orientation	Scanline length (m)	Bed thickness (m)	Fracture sets	Average horizontal spacing (m)	Standard deviation σ (m)
North Head Quarry; SL1	N° 60 E	23.6	1.60	S1, S2	4.18	4.49
				S3, S4	1.95	1.42
North Head Quarry; SL.2	N° 40 W	12.1	1.45	S1, S2	2.88	2.04
				S5, S6	1.07	0.82
North Fleswick Bay; SL3	N° 85 E	14.7	1.30	S1, S2	8.00	2.60
				S3, S4	1.23	1.02
North Fleswick Bay; SL4	N° 5 W	6.9	1.40	S1, S2	3.50	3.00
				S5, S6	1.37	1.05
Fleswick Bay 1; SL5	N° 75 E	11	1.70	S1, S2	2.50	2.30
				S3, S4	1.56	1.35
Fleswick Bay 1; SL6	N° 15 W	11.9	1.70	S1, S2	1.33	0.86
				S5, S6	1.67	1.64
Fleswick Bay 2; SL7	N° 75 E	27.8	1.90	S1, S2	3.65	2.25
				S3, S4	1.73	0.96
Fleswick Bay 2; SL8	N° 15 W	24.2	1.25	S1, S2	3.88	2.14
				S5, S6	1.61	1.44
South Head Cliff; SL9	N° 2 W	13.2	1.30	S1, S2	5.00	2.80
				S5, S6	1.06	0.47
South Head Cliff; SL10	N° 88 E	21.3	1.60	S1, S2	4.50	3.54
				S5, S6	1.49	1.58

Table. 3

Field site/well name	Constant Rate Tests (Recovery phase) Theis, 1926 T (m^2/day)	Step Tests Drawdown phase Eden and Hazel, 1973 T (m^2/day)	Step Tests Flow rates Q (m^3/day)	Step Tests (Recovery phase) Theis, 1926 T (m^2/day)	Upscaled transmissivity T (m^2/day)
Black Ling	135	99	640,870, 1140, 1320, 1440	80	1.09
Bridge End Trial	54	51	734, 834, 1040, 1370, 1520	42	0.99
Ellergill Bridge	53	41	40, 70, 110, 160, 280	35	1.09
Pallaflat Reservoir	51	66	61, 400, 690, 780	-	1.90
Rottington Trial	77	69	370, 780, 1020, 1520, 1910	59	1.44
Thornhilll Trial	754	913	51, 1390, 1740, 20240, 2140, 2220	695	1.40

Table 4.

Layer code	Layer bottom depth (m ASL)	T_{factor}	Layer hydraulic conductivity, K_i (m/day)	Layer far-filed hydraulic head, Δh_i (m)
THORNHILL TRIAL				
L8	14.5	0.21	20.6	-1.1
L7	-2.7	0.12	6.5	-0.5
L6	-14.2	0.05	4.0	0.6
L5	-26.2	0.23	17.5	0.3
L4	-45.9	0.10	4.6	0.4
L3	-59.8	0.10	6.6	0.3
L2	-71.6	0.19	14.7	0.7
L1	-76.5	0.00	0.0	0.3
BRIDGE END TRIAL				
L6	11.6	0.12	0.4	5.0
L5	-23.5	0.05	0.1	3.3
L4	-24.7	0.53	22.5	2.1
L3	-36.4	0.10	0.4	4.9
L2	-44.3	0.21	1.4	3.3
L1	-50.0	0.00	0.0	3.0
BLACK LING				
L4	-14.7	0.2	0.4	-0.34
L3	-22.2	0.1	1.3	0.91
L2	-40.5	0.2	1.1	0.39
L1	-50.0	0.5	5.2	0.03

Table 5.

Layer code	Layer bottom depth (m ASL)	Delta V/Vmax	Layer hydraulic conductivity, K_i (m/day)
PALLAFLAT RESERVOIR			
L4	14.5	0.29	0.4
L3	10.28	0.47	7.4
L2	-14.4	0.24	0.6
L1	-34.0	0.00	0.0
ELLERGILL BRIDGE			
L3	56.76	0.58	1.2
L2	55.14	0.42	10.7
L1	0	0.00	0.0

Table 6.

Reference	Area	Population (n)	Depth interval (m)	Transmissivity (m^2/day)	Flow rates Q (m^3/day)	Test Duration (mins)	Screen length (m)	Borehole diameter (m)
This work	St Bees	6	10 - 159	51 - 754	40 - 2220	650 - 5810	84 - 152	0.15 - 0.2
Allen et al., 1997	St Bees	6	15 - 123	70 - 220	260 - 3740	441 - 87552	35 - 111	0.20 - 0.60
Allen et al., 1997	Carlisle	9	10 - 213	9 - 1268	267 - 1439	2880 - 13325	60 - 201	0.22 - 0.60
Streetly et al., 2000	Sellafield	32	180 - 400	0.46 - 7.8	22 - 65	8640 - 31680	20 - 180	0.54

Table 7.

Highlights

- Contaminant pathways in sandstone aquifers: tectonic vs sedimentary heterogeneities
- Flow in a lithified sandstone is dominated by tectonic fractures (depth ≤180 m)
- Fault structures characterize 50% of water flow in water wells at shallow depth
- Bedding fractures act as main flow conduits in un-faulted wells at shallow depth
- Fracture aperture lack, preserved mineral infills allow matrix flow (depth > 180 m)